Proceedings of Lunar and Planetary Science, Volume 21, pp. 193-219
Lunar and Planetary Institute, Houston, 1991

Geochemistry of 2-4-mm Particles from Apollo 14 Soil (14161) and Implications Regarding Igneous Components and Soil-forming Processes

B. L. Jolliff, R. L. Korotev, and L. A. Haskin

Department of Earth and Planetary Sciences and McDonnell Center for the Space Sciences, Washington University, St. Louis, MO 63130

The lithologic and compositional distributions of 381 2-4-mm particles from sample 14161 cover nearly the entire range of Apollo 14 materials previously reported and include several unusual lithologies, such as quartz monzodiorite, not previously reported or scarce at this site. The distribution of lithologies differs from that found as clasts in the large breccia samples excavated by the formation of Cone Crater, especially by the scarcity of aluminous mare basalt, troctolite, and alkali anorthosite. This indicates that the surface layer of the Fra Mauro Formation was derived from a somewhat different portion of the lunar crust than the level that was excavated by the formation of Cone Crater, as others have also concluded. About 92% of the particles from 14161 are fragments of impact-melt breccias, regolith breccias, fragmental breccias, and impact-melt rocks or glasses. The 2-4-mm particles on average have higher concentrations of incompatible trace elements (ITE) and Na_2O and lower concentrations of CaO than the associated <1-mm fines (14163). Impact-melt breccias are the most abundant particles and are responsible for the high average ITE concentrations. A subset of regolith breccias that includes most of the large agglutinates has compositions nearly identical to that of the <1-mm fine soil, consistent with local derivation by impact of micrometeorites with chondritic siderophile-element ratios. Distributions of ITE in polymict particles from 14161 suggest an origin by mixing of components that have low ITE concentrations with a component that has fixed ITE concentration ratios and high ITE concentrations, possibly greater than those of average high-K KREEP. However, simple mixing with only a few components does not explain the compositions when the concentrations of major elements and compatible trace elements are also considered. The composition of the associated <1-mm fine soil (14163) cannot be obtained by mixing together the compositions of the igneous fragments that are present among the 2-4-mm particles, but it can be closely matched by adding the average composition of the impact-melt breccias to such a mixture. The compositions of the <1-mm fines are modeled as mixtures of some 60% impact-melt breccia, 20-30% noritic lithologies, 5-10% each mare basalt and troctolitic anorthosite, and several tenths of a percent of meteoritic components. With these particular components, mixing models indicate only minor contributions from ferroan or alkali anorthosites and felsite. Based on the results of our modeling, the provenance of the Apollo 14 impact melt breccias contains an igneous component that has high concentrations of FeO, Cr, and Eu relative to the igneous lithologies found among the 2-4-mm particles from 14161, and a La/Yb ratio less than that of KREEP. Mass balance involving the alkali elements constrains the proportion of very-high-K (VHK) basalt in the potential source to be less than 10%.

INTRODUCTION

The Apollo 14 samples include igneous lithologies with unusual compositions (e.g., alkali anorthosites, norites, and felsite; *Shervais,* 1989) compared to the most abundant igneous crustal lithologies found at other lunar sites or in the lunar meteorites. This may in part reflect general compositional differences between the eastern and western nearside highlands as suggested by *Warren and Wasson* (1980). It presumably means that igneous rocks in the source regions of the Apollo 14 materials were significantly different from those at other sample sites. While the differences between Fra Mauro rocks and those from other highland sites are a striking example of such differences, infrared reflectance spectra show unsampled regions of the lunar highlands to be compositionally diverse and probably of different mineralogical makeup from most of the sampled portions. For instance, the western nearside highlands appear to be more gabbroic (i.e., richer in clinopyroxene) than the eastern nearside highlands (dominantly noritic anorthosite) (*Pieters,* 1989).

The "unusual" highland igneous lithologies found at the Apollo 14 site thus deserve close scrutiny so we can estimate their relative crustal abundances, understand how they formed, and determine their relationship to the more typical highland igneous lithologies (i.e., ferroan anorthosite, noritic anorthosite, and Mg-suite plutonic lithologies). Apollo 14 highland igneous rocks, however, are found mainly as rare lithic clasts in breccias (e.g., *Lindstrom et al.,* 1984; *Shervais et al.,* 1985a; *Goodrich et al.,* 1986; *Neal et al.,* 1988). Crystalline and fragmental matrix breccias and regolith breccias make up the bulk of the Apollo 14 samples, and these are the principal sources of information on the composition of the portions of the lunar crust that were sampled by their formation.

As a result of the spreading and mixing effects of impact cratering, lunar soils contain rock fragments from large areas and sections of lunar crust. We have systematically analyzed 381 unsorted, 2-4-mm particles to determine the compositions and lithologies of fragments in that size range, to determine in what proportion each occurs, and to search for unusual rock types and compositions. Our objectives include the determi-

nation of the following: (1) which igneous lithologies found as clasts in the larger breccia samples are also represented among the soil fragments; (2) from which igneous lithologies do the Apollo 14 soils mainly derive; (3) what lithologic components cause the compositional trends among Apollo 14 polymict materials; and (4) how the 2-4-mm particles relate to the remainder of the soil and to constructional and destructional processes of soil formation. With regard to the last objective, we find it necessary to draw comparisons between samples 14161 (2-4-mm) and 14163 (<1 mm), which represent a submature to mature soil, and samples 14141 (<1 mm) and 14143 (2-4 mm), which is an immature soil (*Morris,* 1976) collected at the rim of Cone Crater.

In this paper we describe the compositional systematics of 381 particles that we have analyzed from 14161, which was taken near the lunar module (LM) as part of the bulk sample, 14160-14163. Lithologic descriptions are based on petrographic observations of thin sections of 106 of these particles. Detailed work on subsets of these particles will be presented elsewhere (e.g., *Jolliff,* 1991). In this paper, we discuss the distribution of lithologies, based on petrographic examination and compositions determined by INAA, and implications of the compositions of polymict particles regarding igneous precursors and soil-forming processes. We also present compositional data on <1-mm soil 14141 and an average for ~40 1-4-mm particles from 14142/3 for comparison to the particles from 14161.

ANALYTICAL PROCEDURES

Particles were chosen for analysis without any petrographic preselection criteria so as not to bias the lithologic distribution, but were grouped according to mass in a given neutron activation set to optimize gamma-ray detection efficiency. Individual particles were rinsed by gentle ultrasonic cleaning in freon to remove most of the dust and fine soil coating without disaggregating the more friable breccias. Each particle was examined under a binocular microscope for a preliminary petrographic classification, then weighed and sealed in a high-purity silica tube for irradiation. Sample masses range from 7 to 117 mg.

Instrumental neutron activation analysis (INAA) methods are essentially those described by *Korotev* (1991) and data reduction was done using versions of the TEABAGS program (*Lindstrom and Korotev,* 1982), revised to operate on a DEC MicroVAX II computer. Samples and synthetic glass standards were irradiated at the University of Missouri research reactor for 48 hours with a thermal neutron flux of 5×10^{13} $cm^{-2}sec^{-1}$. Individual particles were radioassayed initially for 1-2 hr. Three minutes after acquisition of data for a fragment, we obtained preliminary concentrations of some 22 elements. Concentrations of these elements were compared by computer to those in a catalog of compositions of Apollo 14 materials to provide a compositional classification and to quickly identify compositionally unusual particles. With the exception of a small percentage of the most common lithologies, nearly all the particles were assayed a second time, and the most unusual particles received more extensive assay by our normal procedures. Average analytical uncertainties are as follows: 1-3%—Na_2O, Sc, Cr, FeO, Co, Zr, La, Sm, Eu, Tb, Yb, Lu, Hf, Ta, Th; 4-7%—Ba, Cs, U; 8-10%—CaO, Ni; 10-20%—Ir, Au. For those particles that received only one assay, the following analytical uncertainties apply: 6-8%—Eu; 30-40%—Ni, Ir.

After allowing the radioactivity to decay for several months, thin sections of selected particles were made for detailed petrographic study and mineral analysis using a JEOL 733 electron microprobe. Of the 381 particles analyzed by INAA, thin sections were made of 106; potted butts exist for most, and for about half of the sectioned particles, a small mass of free sample remains.

RESULTS

Lithologic and Compositional Distribution

Based on examination with the binocular microscope, on thin-section petrography on a subset, and on compositional data obtained by INAA, we classified each particle into one of four broad groups: impact melt lithologies, fragmental breccias, regolith breccias, and igneous or monomict lithologies (Fig. 1). These groups correlate with those used in previous classifications and some specific correlations are given in the following sections. We have attempted to follow the nomenclature recommended by *Stöffler et al.* (1980), who give an excellent cross-reference for nomenclature used in earlier papers. By classifying a particle as igneous, we do not imply strict compositional pristinity in the sense of *Warren and Wasson* (1977). Rather, our use of the term igneous indicates that the composition and/or texture of the particle is dominated by a particular igneous component.

Impact melt lithologies. These particles have been subdivided into impact-melt breccias (IMBx), impact-melt rocks that have no clasts (IMR), and impact-melt glasses (IMGl). The most abundant (~40 wt% of the entire sample, see Fig. 1) are impact-melt breccias, which correspond to the (1) recrystallized breccias of *McKay et al.* (1972), (2) F4 breccias of *Wilshire and Jackson* (1972), (3) medium to high grade, groups 4-7 of *Warner* (1972), (4) annealed breccias of *Quaide and Wrigley* (1972), (5) recrystallized noritic breccias of *Taylor et al.* (1972), and (6) recrystallized noritic, poikilitic, and crystalline breccias of *Simon et al.* (1982). *McKay et al.* (1972) classified 41% of the 1-4-mm particles in 14161/2 as recrystallized breccias compared to our 33% (40 wt%, Fig. 1) for the impact-melt breccias. These breccia fragments consist of very fine-grained crystalline or recrystallized matrix and coarser mineral and lithic clasts (e.g., Figs. 2a-d). Mineral clasts are more common than lithic clasts and mostly consist of plagioclase, low-Ca pyroxene, and partially resorbed olivine, in order of abundance. A range of matrix textures is observed among these particles: Most are finely granular to subophitic (Figs. 2a,b), although in many the pyroxenes (mostly pigeonite) have developed ophitic to incipiently poikilitic or poikiloblastic textures (Figs. 2c,d). There is a subset of particles with medium-grained (300-μm to 3.0-mm) poikilitic pyroxene that is referred to as "granulitic" in Table 1. These probably correspond to "granulitic noritic breccias" of *Taylor et al.* (1972). A common feature of the matrix mineralogy and fabric of most of the impact-melt breccias is the rather uniform distribution of very-fine-grained

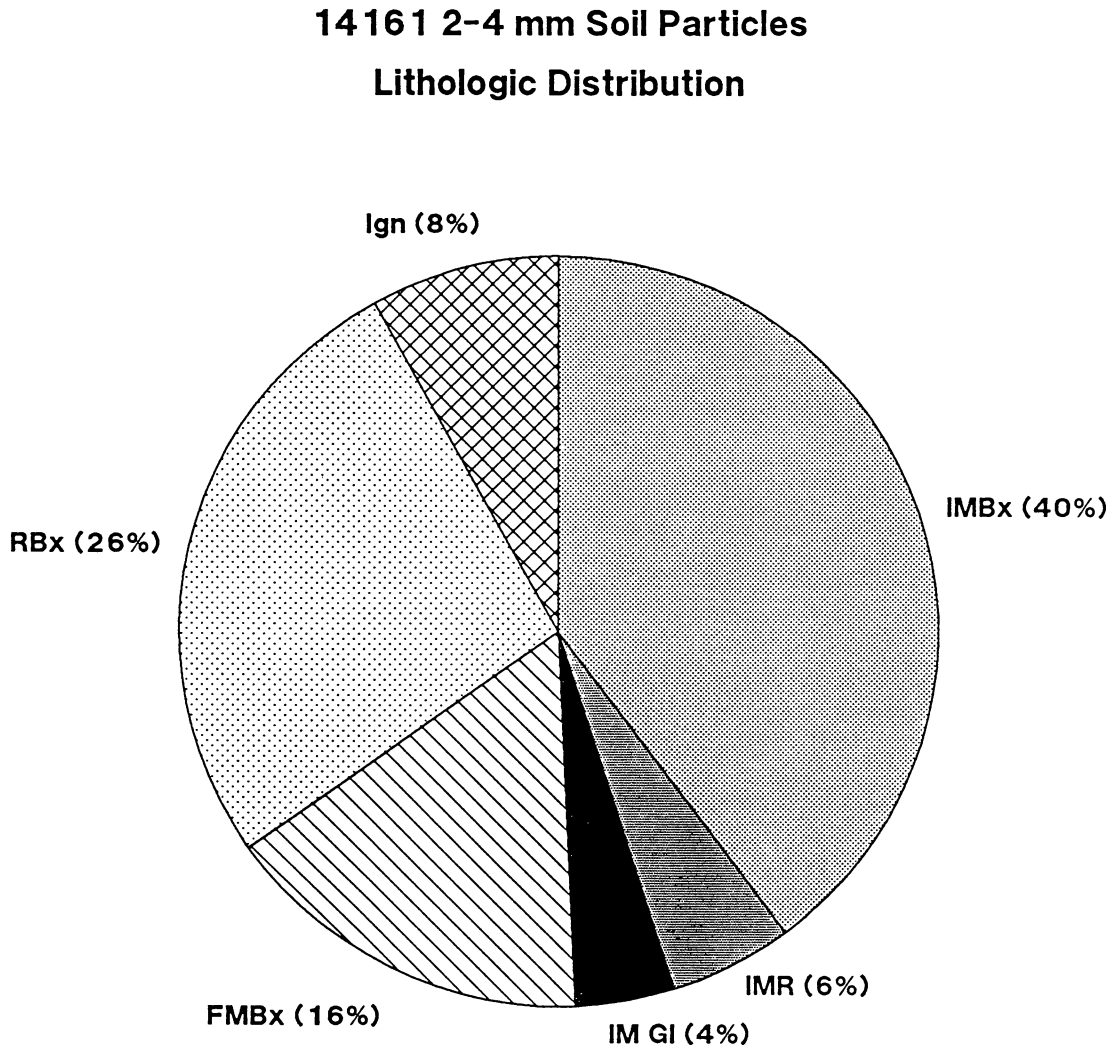

Fig. 1. Summary of compositional and lithologic classification of 2-4-mm particles from 14161, normalized to particle masses. Determinations based on compositional data by INAA combined with binocular microscope observations and thin-section petrography on a subset of particles. Ign = igneous, IMBx = impact-melt breccias, IMR = impact-melt rocks, IM Gl = impact-melt glasses, FMBx = fragmental matrix breccias, RBx = regolith breccias and agglutinates.

ilmenite (cf. *Taylor et al.,* 1972, p. 996), although a subset of the impact-melt breccias developed fine- to medium-grained ilmenite oikocrysts (Fig. 2d). On the basis of matrix texture and mineralogy and, consequently, the macroscopic features such as color and surface texture, the impact-melt breccias can be subdivided into light and dark IMBx. Judging by macroscopic appearance, one might expect compositional differences that correlate with these groupings; however, as shown below, this is not the case. Most of the IMBx are noritic in composition (8-11.5 wt% FeO, 8-12 wt% CaO) and they have, on average, high incompatible-trace-element (ITE) concentrations (Table 1—Zr, Hf, Cs, Ba, REE, Ta, Th, U). Previous classifications have distinguished low-temperature or low-grade breccias from high-temperature or high-grade breccias based on criteria such as porosity (e.g., *Taylor et al.,* 1972; *Warner,* 1972); however, correlations with compositional variations between these groups are weak. On the basis of trace-element compositional variations, however, the impact-melt breccias are diverse. On the basis of groupings of Sm and Sc concentrations of melt rocks, other workers have tentatively identified the products of different melt sheets (e.g., *Laul et al.,* 1989, and references therein). On a plot of Sm vs. Sc/Sm,

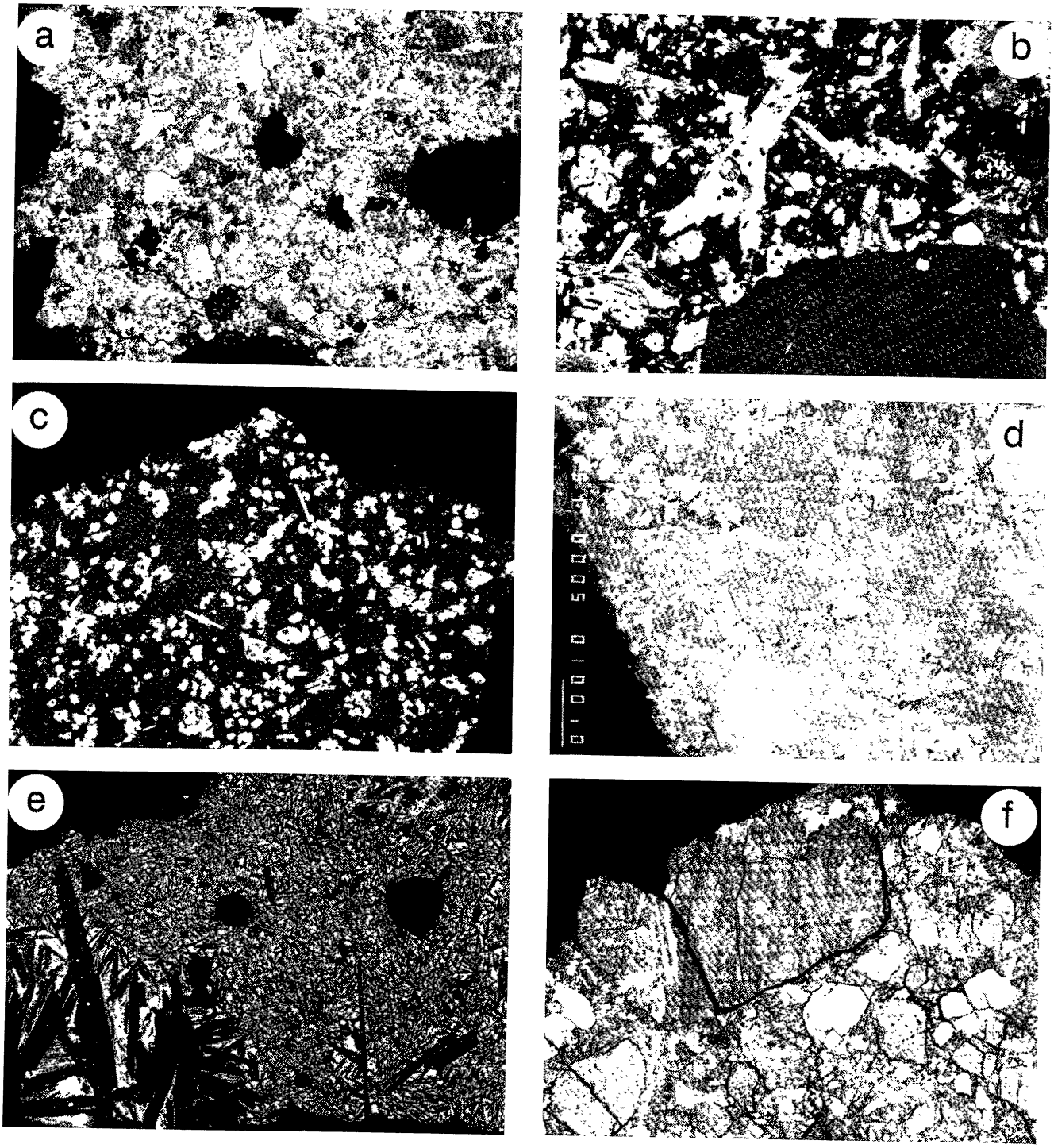

Fig. 2. Photomicrographs of some representative 2-4-mm particles from 14161. In backscattered-electron images (BEI), the dark gray material is generally plagioclase, medium gray is pyroxene, lighter gray is olivine, and white is ilmenite or an accessory mineral such as zircon, phosphates, troilite, or metal. **(a)** 14161,7070 impact-melt breccia, BEI. This breccia is relatively porous and has clasts of plagioclase, olivine, and pyroxene in a very fine-grained matrix of plagioclase and pyroxene. Olivine clasts are mantled by pyroxene. Ilmenite and accessory minerals are evenly distributed throughout the matrix. Field of view ~1.5 mm. **(b)** Matrix of IMBx ,7086 at high magnification (BEI, field of view ~350 μm). Interstitial glass occurs between very-fine-grained plagioclase laths. Bright phases are ilmenite, whitlockite, and zircon. **(c)** Fine-grained, incipiently poikiloblastic impact-melt breccia ,7014 (BEI, 1.6 mm). **(d)** Fine- to medium-grained, poikiloblastic breccia (BEI); note ilmenite poikiloblast at right and 100-μm ilmenite with baddeleyite core, lower center. **(e)** Very-fine-grained, intersertal impact-melt rock ,7042 (BEI, ~1.5 mm). The coarsest mafic grains are mostly olivine and the finer grains are mostly pyroxene. Note rounded vesicles. **(f)** Fragmental QMD breccia ,7073 (BEI, ~1 mm). Clast in upper center is a granophyric intergrowth of silica (dark gray) and feldspars (lighter gray).

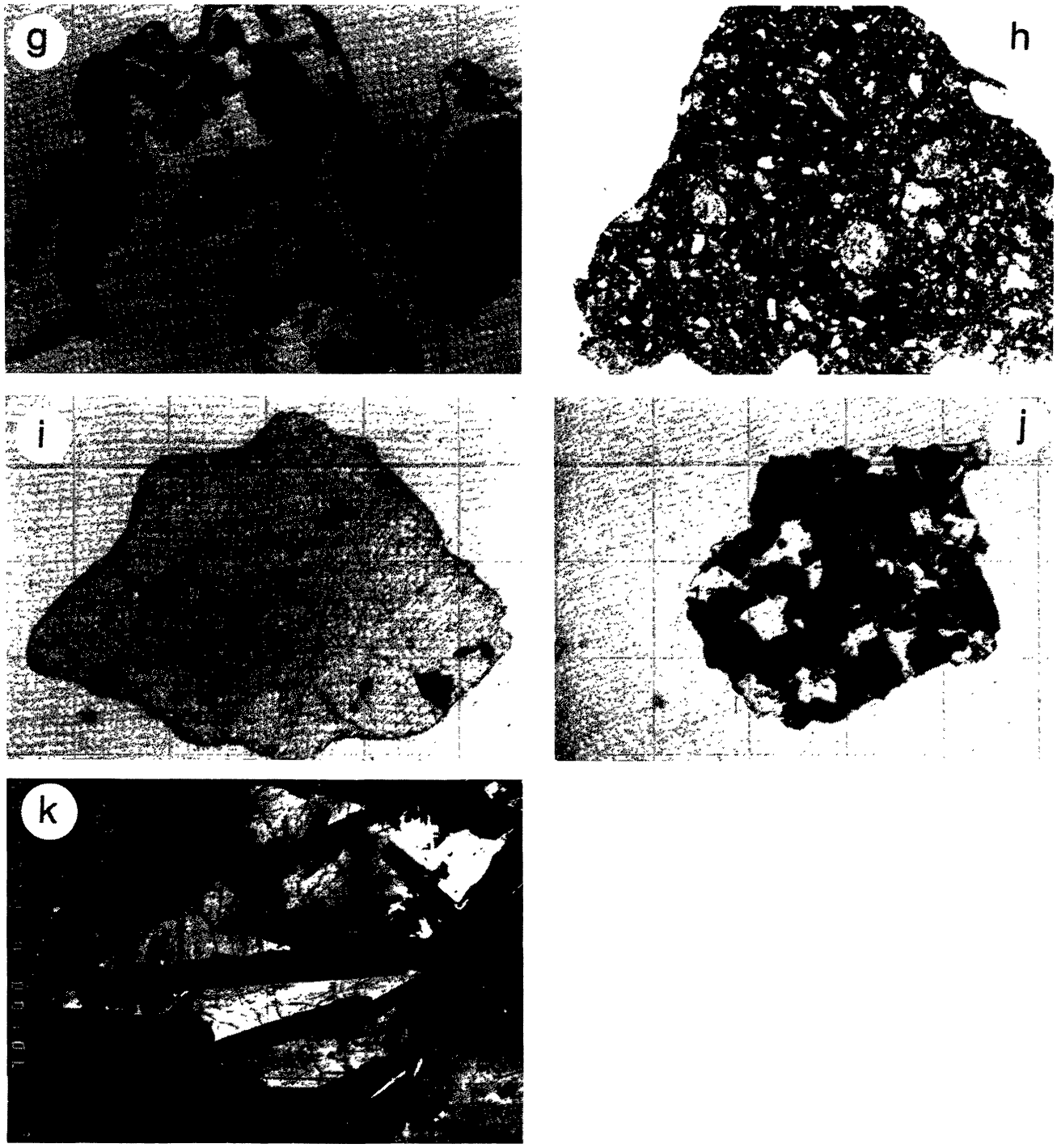

Fig. 2. (continued) **(g)** Impact-melt glass ,7148, partially devitrified, transmitted light, plane polarized (TL, PP), ~1.6 mm. **(h)** Regolith breccia ,7003 (TL, PP, ~3.3 mm). Note rounded lithic and glass clasts. **(i)** Ferroan anorthosite fragment ,7033 (TL PP, ~3.3 mm), consisting of ~12 individual plagioclase crystals and scattered pyroxene crystals (dark). **(j)** Norite fragment ,7080 (TL, PP, ~3.3 mm). Mafic mineral grains are mostly low-Ca pyroxene. Plagioclase is completely isotropic. **(k)** Intersertal KREEP basalt ,7062 (BEI, ~1.5 mm), interstitial material is mostly pyroxene, zoned from very magnesian (medium gray) to Fe-rich (light gray) compositions. Bright phase is mainly ilmenite.

TABLE 1. Impact-melt (crystalline matrix) breccias and granulitic (poikiloblastic and granoblastic) breccias.

Specific	INAA	Na_2O	CaO	Sc	Cr	FeO	Co	Ni	Zr	Cs	Ba	La	Sm	Specific
,7204	219.030	0.35	16.1	8.9	825	4.70	16.8	176	33	0.05	29	2.00	1.00	,7204
,7032	212.042	0.43	9.8	20.5	1510	10.14	23.9	163	340	0.32	362	23.8	10.8	,7032
,7058	212.078	0.60	9.5	13.5	1264	10.15	69.5	910	640	0.3	537	44.8	19.4	,7058
,7275	219.114	0.84	8.7	19.6	1132	9.18	25.9	204	620	1.8	987	45.4	19.7	,7275
,7081	212.101	0.86	11.2	20.4	1111	8.27	19.3	132	700	0.9	900	45.1	19.8	,7081
,7111	216.011	0.71	9.4	14.7	1240	9.49	49.3	600	840	0.6	730	52.3	22.4	,7111
,7014	212.024	0.84	11.7	13.1	764	6.87	13.3	<dl	1050	0.9	1010	70.6	30.4	,7014
,7005	212.015	0.78	10.6	20.9	1162	9.18	23.1	<350	970	0.7	840	71.2	32.6	,7005
,7072	212.092	0.67	8.6	27.5	1680	12.73	40.7	370	1050	0.16	620	76.4	33.9	,7072
,7070	212.090	0.73	9.6	18.9	1130	9.79	39.9	440	1080	0.44	870	76.8	34.0	,7070
,7059	212.079	0.77	10.1	23.9	1460	10.56	35.7	290	1050	0.48	850	75.4	34.1	,7059
,7068	212.088	0.70	9.3	21.0	1350	9.78	29.8	160	1150	0.6	950	80.6	35.5	,7068
,7053	212.073	0.85	10.4	19.5	1178	10.45	81.8	1000	1210	0.8	910	81.2	35.8	,7053
,7184	219.010	0.82	10.5	23.6	1279	10.78	31.5	250	1270	0.9	980	83.0	37.2	,7184
,7186	219.012	0.83	11.3	17.0	1245	8.45	10.7	<70	1090	0.50	742	84.8	38.9	,7186
,7028	212.038	0.86	9.7	19.0	1039	9.25	28.3	300	1350	0.7	960	90.5	39.4	,7028
,7126	216.035	0.82	10.8	22.2	1267	10.80	34.9	300	1850	0.7	1050	93.7	40.2	,7126
,7085	212.105	0.77	10.7	26.7	1390	11.72	37.2	320	1300	0.49	790	93.5	40.2	,7085
,7052	212.072	0.81	9.5	20.7	1205	11.45	56.9	700	1300	0.9	1040	92.1	40.5	,7052
,7087	212.107	0.82	10.5	19.9	1130	9.65	30.7	440	1900	0.9	1010	97.0	42.8	,7087
,7181	216.090	0.85	8.7	21.0	1207	10.65	38.0	260	1330	0.6	1030	99.8	43.8	,7181
,7164	216.073	0.90	10.0	21.5	1152	10.74	39.0	350	1560	0.37	990	98.9	44.2	,7164
,7047	212.057	0.88	10.6	21.3	1189	11.26	30.1	340	1420	0.6	1160	103	44.3	,7047
,7137	216.046	0.81	7.9	18.0	1023	10.17	29.1	420	1400	0.8	860	103	45.3	,7137
,7043	212.053	0.74	10.4	26.2	1544	11.16	31.1	280	1700	0.7	800	104	45.5	,7043
,7108	216.008	0.86	9.6	22.5	1198	10.82	32.4	280	1750	0.8	1240	106	45.7	,7108
,7163	216.072	0.86	11.2	18.2	1145	7.40	13.4	42	1180	1.1	900	103	46.3	,7163
,7125	216.034	1.15	11.6	17.3	823	9.11	26.5	240	1480	0.29	874	108	46.7	,7125
,7060	212.080	0.84	9.3	19.7	1007	9.90	32.9	350	1540	1.6	1330	109	47.5	,7060
,7100	212.120	0.62	8.2	22.0	1401	12.90	23.7	190	1430	0.48	730	127	58.0	,7100
,7086	212.106	0.89	8.8	20.4	1109	10.24	42.4	390	2020	1.9	910	145	62.0	,7086

the compositions of impact-melt breccias from 14161 cover a range of magnitude exceeding that which encompasses at least five presumably distinct groups of Apollo 15 melt rocks (*Ryder and Spudis,* 1987). It is uncertain whether such a broad range of compositions reflects multiple melt sheets or whether it reflects a single very large, complex, and heterogeneous melt sheet. Individual small samples of impact-melt breccia fragments from a single large rock, 14305, have compositions that cover about half the range of the suite of impact-melt breccia particles from 14161 (unpublished data from our lab).

Chondrite-normalized REE patterns are illustrated in Fig. 3 for one group of "light" IMBx particles that macroscopically appear to be very similar to one another. Their REE concentrations range from about the level of the associated <1-mm fines (14163) to levels in excess of those given for "average high-K KREEP" (*Warren,* 1989). The mean composition of this group of IMBx is about the same as the mean of the entire suite of IMBx in 14161, and is taken as representative of the most abundant IMBx particles. This IMBx composition is compared to that of the <1-mm fines (14163) and to the weighted mean of the 2-4-mm particles in Fig. 4 (see also Table 6). The impact-melt breccias have higher average Na_2O and ITE concentrations but lower Ca and Cr

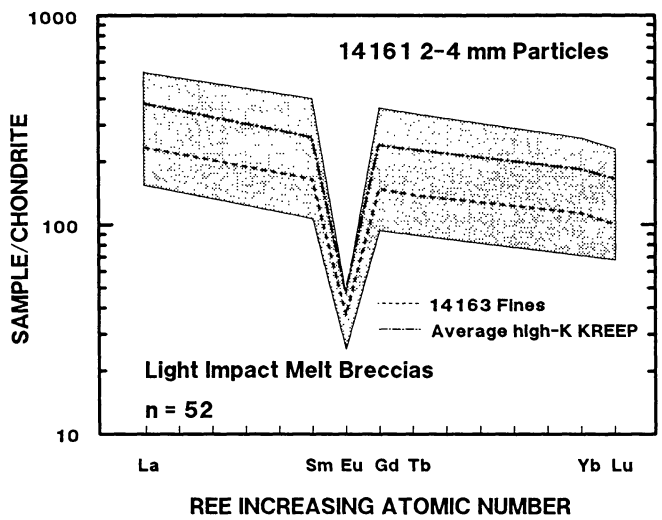

Fig. 3. Range of rare earth element concentrations in the light impact-melt breccia group. The dashed line is the composition of the associated <1-mm fines, 14163. Average high-K KREEP (*Warren,* 1989) shown for comparison.

TABLE 1. (continued).

Specific	Eu	Tb	Yb	Lu	Hf	Ta	Ir	Au	Th	U	Mass	Description	Specific
,7204	0.77	0.22	0.86	0.130	0.77	0.1	7.6	3	0.3	0.11	43.5	GBx, poik	,7204
,7032	1.60	2.46	12.0	1.70	8.73	0.8	5.9	<dl	4.4	1.2	25.5	GBx, poik	,7032
,7058	2.38	3.9	14.7	2.04	15.2	2.1	20.8	19.5	9.4	2.7	28.5	IMBx	,7058
,7275	2.53	4.1	17.1	2.40	16.0	2.3	5.2	5.3	10.4	3.1	35.2	IMBx	,7275
,7081	2.57	4.2	17.4	2.40	16.8	2.4	3	<6	8.9	2.6	15.7	IMBx	,7081
,7111	2.49	4.5	17.4	2.40	20.1	2.3	11.6	9	10.7	3.2	76.8	IMBx	,7111
,7014	1.80	5.9	23.7	3.23	25.6	2.9	<dl	<5	16.5	4.4	18.0	GBx, poik	,7014
,7005	2.70	6.2	25.2	3.42	23.8	2.8	<dl	<8	12.6	3.6	14.6	IMBx	,7005
,7072	2.51	6.7	22.5	3.09	24.7	2.9	8.8	13	12.7	2.9	14.8	IMBx	,7072
,7070	2.62	6.8	24.9	3.36	25.7	3.3	12	14	14.9	4.2	27.0	IMBx	,7070
,7059	2.57	7.0	25.5	3.52	26.1	3.4	<24	<10	15.5	4.3	20.6	IMBx	,7059
,7068	2.34	7.0	26.2	3.62	27.3	3.5	<dl	<9	16.6	4.4	28.0	IMBx	,7068
,7053	2.82	7.1	25.9	3.48	27.8	3.2	26	23	15.3	4.2	24.7	IMBx	,7053
,7184	2.76	7.4	27.7	3.77	31.3	3.8	<18	8	17.1	4.8	57.4	IMBx	,7184
,7186	3.01	7.3	23.4	3.17	25.9	1.9	<4	<4	9.7	2.7	46.7	GBx, poik	,7186
,7028	2.97	7.7	28.7	3.98	29.3	4.1	10	<10	17.2	4.8	18.6	IMBx	,7028
,7126	2.75	8.2	31.1	4.30	42.3	4.4	7.7	8	19.8	5.6	31.6	IMBx	,7126
,7085	2.74	8.0	27.8	3.84	29.3	3.8	12	<12	16.6	4.2	14.8	IMBx	,7085
,7052	2.67	8.2	29.2	3.93	31.1	3.8	17.2	15	17.0	4.8	27.9	GBx, poik	,7052
,7087	2.90	8.2	30.7	4.19	34.2	3.8	<24	6	18.3	4.6	17.3	IMBx	,7087
,7181	2.90	8.7	31.1	4.31	32.8	4.0	18	9	18.2	5.2	24.0	IMBx	,7181
,7164	3.47	8.8	32.4	4.46	38.7	4.1	11	4.4	17.2	4.5	21.8	GBx	,7164
,7047	2.74	8.9	32.6	4.49	34.1	4.4	7.6	11	20.3	5.9	21.1	IMBx	,7047
,7137	2.62	8.8	29.8	4.07	35.5	3.5	<17	<6	17.5	4.1	29.4	GBx	,7137
,7043	2.49	8.8	30.3	4.13	38.2	4.0	4.9	9	18.8	5.2	28.1	IMBx	,7043
,7108	2.78	9.3	33.4	4.53	37.0	4.8	<13	9	20.5	6.3	78.2	IMBx	,7108
,7163	2.56	9.4	30.8	4.21	29.6	2.7	<dl	<5	16.7	4.2	18.4	IMBx	,7163
,7125	3.89	9.5	33.5	4.64	35.9	4.5	5.8	3.8	19.9	0.1	40.4	GBx	,7125
,7060	2.98	9.5	34.6	4.74	35.9	4.6	8.2	7	21.5	6.0	24.8	IMBx	,7060
,7100	2.34	10.7	32.0	4.24	33.8	3.6	5	8	16.8	3.3	22.7	GBx, poik	,7100
,7086	2.78	12.3	41.1	5.55	47.8	5.1	8.7	<13	25.6	5.8	18.5	IMBx	,7086

Na_2O, CaO, and FeO in % (cg/g, total element as oxide); Au and Ir in ppb (ng/g); all other values in ppm (μg/g). "<dl" = below detection limit (no concentration value obtained) and no upper limit estimate made. Uncertainties are given in section on Analytical Procedures. IMBx: noritic impact-melt breccia (crystalline matrix); GBx: granulitic breccia (poikiloblastic or granoblastic matrix).

concentrations than the bulk <1-mm fines and the mean of the 2-4-mm particles. They have lower average Sc, Fe, and Co concentrations than the <1-mm fines, but greater than average concentrations of these elements in the 2-4-mm particles. The ITE-enriched compositions of the impact-melt breccias are manifested in the mineralogy of the "melt" matrix, which, in addition to pyroxene, typically includes relatively sodic plagioclase (An_{72}-An_{82}), whitlockite, apatite, barian K-feldspar, and zircon.

Particles classified on textural grounds as "impact-melt rocks" (IMR) are fine-grained, crystalline, relatively homogeneous, and contain no discernable clasts, but have obvious meteoritic contamination as indicated by their siderophile-element concentrations (Table 2). They are fine grained (30-300 μm) to very fine grained (<30 μm) and have an intersertal basaltic texture (Fig. 2e). Compositionally and texturally, several of these particles are similar to LKFM basalts, such as 14276 and 14310 (summarized by *Vaniman and Papike,* 1980). One IMR (14161,7233) has extremely high ITE concentrations (~3 × average high K-KREEP) and sodic plagioclase (An_{63-69}), but relatively magnesian pyroxene [Mg/(Mg + Fe): 0.64-0.71]. Its texture is fine to very fine grained, subophitic to "sheath-like," similar to the group 8 texture described by *Warner* (1972) for sample 14068.

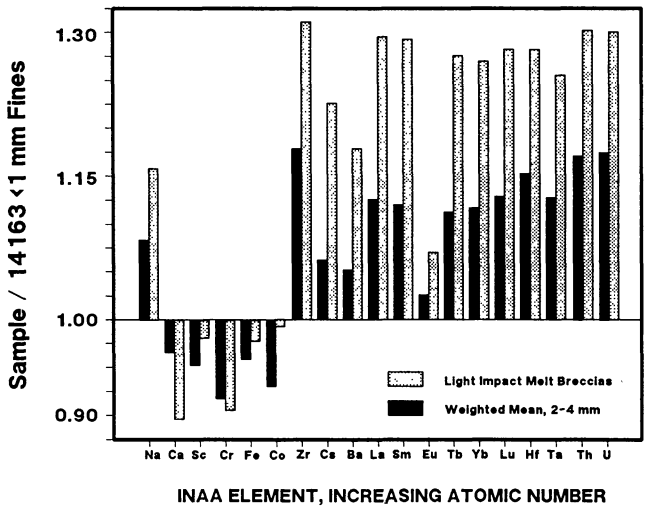

Fig. 4. Comparison of the weighted mean composition of 381 2-4-mm particles from 14161 (dark) and the average impact-melt breccia composition (shaded), normalized to the associated <1-mm fine soil.

TABLE 2. Glassy melt breccias, impact glasses, and impact-melt rocks.

Specific	INAA	Na_2O	CaO	Sc	Cr	FeO	Co	Ni	Zr	Cs	Ba	La	Sm	Specific
,7050	212.060	0.07	14.6	11.1	832	5.86	17.4	49	83	<0.06	77	6.31	2.92	,7050
,7148	216.057	0.22	14.7	12.0	998	6.22	21.9	128	102	0.11	83	7.23	3.32	,7148
,7116	216.016	0.28	14.0	13.9	10.7	6.98	25.7	220	280	0.17	205	17.1	7.8	,7116
,7127	216.036	0.55	10.4	43.4	1870	19.70	46.6	260	510	0.23	350	32.6	16.3	,7127
,7202	219.028	0.72	13.0	18.2	1122	8.07	21.1	190	670	0.34	519	48.6	22.0	,7202
,7042	212.052	0.73	14.2	18.9	1112	8.34	26.4	240	1010	0.7	690	57.5	25.3	,7042
,7055	212.075	0.70	9.7	14.3	857	9.65	23.8	<260	770	<1.0	610	67.1	29.5	,7055
,7021	212.031	0.93	8.7	18.0	830	11.10	25.4	<290	2350	0.8	1360	78.1	33.7	,7021
,7144	216.053	0.96	12.7	17.3	884	7.65	17.0	100	1430	0.6	998	78.7	33.7	,7144
,7178	216.087	0.88	11.0	20.3	1277	10.06	32.4	320	1220	0.9	1100	86.6	38.6	,7178
,7175	216.084	1.09	11.5	18.6	790	8.38	15.0	90	1850	1.1	1420	104	45.3	,7175
,7233	219.059	0.80	12.5	41.4	1144	9.34	41.9	360	4760	3.0	3250	325	150	,7233

TABLE 2. (continued).

Specific	Eu	Tb	Yb	Lu	Hf	Ta	Ir	Au	Th	U	Mass	Description	Specific
,7050	0.85	0.61	2.27	0.31	2.22	0.28	6.9	<2.3	1.1	0.24	26.1	Troc Gl	,7050
,7148	0.89	0.66	2.59	0.346	2.38	0.32	15.2	1.7	1.3	0.37	20.2	IM Gl	,7148
,7116	1.17	1.55	5.8	0.78	6.50	0.73	15.3	<3.8	3.3	0.88	22.6	IM Gl	,7116
,7127	1.96	3.4	12.2	1.66	12.9	1.6	8.4	<2.7	5.4	1.4	34.2	Mbas Gls	,7127
,7202	1.85	4.4	15.8	2.19	17.1	2.1	9	<6	8.6	2.6	66.5	IMR	,7202
,7042	2.21	5.1	18.8	2.55	20.4	2.5	<14	<6	10.6	3.3	21.0	IMR	,7042
,7055	2.20	5.8	20.8	2.83	20.7	2.6	<dl	<4	12.6	3.9	21.1	Gl MBx	,7055
,7021	3.10	6.8	26.7	3.73	53.3	3.5	<dl	<6	16.0	4.4	15.5	Gl MBx	,7021
,7144	3.58	6.8	25.5	3.58	33.4	3.4	<4.7	<5	15.8	4.1	15.3	Gl MBx	,7144
,7178	2.65	7.8	28.3	3.76	29.9	4.2	5.1	<9	17.7	4.6	14.2	Gl MBx	,7178
,7175	3.65	9.2	34.2	4.74	43.9	4.6	2.3	<3	22.1	6.3	23.0	Gl MBx	,7175
,7233	4.34	30	101	13.8	112	12.0	<17	<13	50.8	14.4	42.5	IMR	,7233

Na_2O, CaO, and FeO in % (cg/g, total element as oxide); Au and Ir in ppb (ng/g); all other values in ppm (μg/g). "<dl" = below detection limit (no concentration value obtained) and no upper limit estimate made. Uncertainties are given in section on Analytical Procedures. Gl MBx: glassy melt breccia, no obvious regolith components; IMR: impact-melt rock, no clasts; IM Gl: impact melt glass.

There is a small group of impact-melt glasses that consists of glass beads, ropy glass particles, vitric fragments, and clast-poor, glassy-matrix melt breccias (e.g., Fig. 2g). The glasses have a broad range of compositions and include two with mare basalt compositions, several with troctolitic or noritic compositions, and others with KREEP-like compositions (Table 2). Several particles that are partly glassy have anorthositic compositions and low siderophile-element concentrations. The latter are grouped with the igneous particles.

Fragmental-matrix breccias. Fragmental-matrix breccias (FMBx) appear to have fragmental rather than crystalline matrices (e.g., Fig. 2f). These breccias are difficult to distinguish macroscopically from cohesive regolith breccias or heavily fractured IMBx. In thin section, the absence of fine-grained soil components such as glass clasts distinguishes these from regolith breccias, and their matrix textures distinguish them from "typical" IMBx. Most of the FMBx have a continuous distribution of clast sizes from the largest clasts to the matrix (<30 μm). However, even the slightest recrystallization or annealing of the matrix makes the fragmental interpretation ambiguous. Compositionally, the fragmental breccias overlap broadly with the crystalline matrix breccias but, on average, they appear to have slightly lower ITE concentrations because they lack the ITE-rich melt matrix, except where present in IMBx clasts within the fragmental breccia. *McKay et al.* (1972) reported 30% "vitric" breccias in 14161/2; these correspond to our fragmental breccias and our "nonagglutinitic" regolith breccias (see below), which comprise some 31% (by number) of fragments (24 wt%). Some of the fragmental breccias are compositionally similar to known igneous rock types, indicating that they have been mostly fractured (cataclastic), but not necessarily mixed to the extent that IMBx were. Examples include anorthositic norite, norite, monzogabbro, and quartz monzodiorite cataclastic breccias (Table 3).

Regolith breccias and agglutinates. Particles classified as regolith breccias (RBx) consist of partially fused or compacted soil with variable amounts of glassy matrix or macroscopically (or microscopically) observable regolith components (e.g., Fig. 2h). Some of these particles are large agglutinates (or fragments thereof), and others appear to be fragments of larger regolith breccias such as 14301 or 14313. The regolith breccias may be divided into two groups. One (group A, which includes agglutinates) contains particles that consist of compacted soil bound and mixed in different proportions with frothy, vesicular glass. These particles include some that are single, large agglutinates, some that are compacted soil with little glass, and a complete range of

TABLE 3. Fragmental matrix and other breccias.

Specific	INAA	Na_2O	CaO	Sc	Cr	FeO	Co	Ni	Zr	Cs	Ba	La	Sm	Specific
,7129	216.038	0.54	13.5	13.8	863	6.73	13.4	68	690	0.52	491	41.5	18.3	,7129
,7151	216.060	0.59	14.5	11.6	679	5.33	9.8	44	690	0.7	499	44.6	19.7	,7151
,7105	216.005	0.58	11.6	14.1	991	6.72	25.1	<147	1760	0.30	513	38.8	16.5	,7105
,7136	216.045	0.63	11.6	11.8	796	6.44	12.6	90	610	0.8	742	38.3	16.6	,7136
,7034	212.044	0.63	8.7	15.6	1349	10.53	69.1	870	760	0.8	670	50.9	22.2	,7034
,7170	216.079	0.98	11.3	15.3	1059	6.91	12.8	45	1260	1.3	940	55.6	25.0	,7170
,7054	212.074	0.77	8.7	20.6	1270	10.63	29.0	<300	1660	0.7	1060	93.0	41.4	,7054
,7038	212.048	1.03	12.7	19.4	921	9.42	21.1	150	1750	1.1	1300	126	53.5	,7038
,7264	219.103	0.71	13.2	33.2	1203	9.27	22.4	230	2590	1.0	1690	154	73.3	,7264
,7073	212.093	1.14	8.7	28.2	612	13.20	9.2	<110	2950	0.6	1910	198	86.7	,7073

TABLE 3. (continued).

Specific	Eu	Tb	Yb	Lu	Hf	Ta	Ir	Au	Th	U	Mass	Description	Specific
,7129	1.41	3.8	14.3	1.99	16.7	2.3	4.1	<2	8.8	2.5	28.4	AN Bx	,7129
,7151	1.51	4.0	14.3	1.92	16.6	2.2	3.4	<3.5	9.3	2.3	23.9	AN Bx	,7151
,7105	2.21	3.2	13.0	1.82	39.2	1.5	4.3	<5	7.5	2.1	72.5	FMBx	,7105
,7136	1.72	3.4	14.3	1.96	15.5	2.2	3.4	<3.8	10.4	2.8	24.5	NO FMBx	,7136
,7034	2.22	4.5	17.0	2.33	17.2	2.4	15.7	11.3	10.4	2.9	21.3	FMBx	,7034
,7170	2.75	5.2	20.2	2.81	29.3	2.4	4.8	<5	10.9	3.1	22.4	NO FMBx	,7170
,7054	2.58	8.6	31.5	4.39	38.4	4.5	<21	<10	20.1	5.3	25.7	FMBx	,7054
,7038	3.68	10.9	39.5	5.43	41.2	4.7	4.9	<8	23.2	6.1	33.3	FMBx	,7038
,7264	2.47	14.9	51	6.94	60	6.4	<dl	<7	30.4	8.5	25.3	MG FMBx	,7264
,7073	3.10	17.5	63	8.70	71	7.9	<7	<7	41.1	11.3	9.7	QMD FMBx	,7073

Na_2O, CaO, and FeO in % (cg/g, total element as oxide); Au and Ir in ppb (ng/g); all other values in ppm (μg/g). "<dl" = below detection limit (no concentration value obtained) and no upper limit estimate made. Uncertainties are given in section on Analytical Procedures. FMBx: fragmental matrix breccia; NO, MG, QMD: norite, monzogabbro, quartz monzodiorite; AN: anorthositic norite breccia.

intermediate mixtures of soil and glass. These are petrographically and compositionally very similar to one another and to the <1-mm fines (14163), although on average, they have slightly higher siderophile-element concentrations than the fine soil (Table 4). This group comprises about 18% (by number) of our sample of 14161 (cf. 13% agglutinates, *McKay et al.,* 1972). The other group includes all other regolith breccia particles and is petrographically and compositionally more diverse than group A regolith breccias and agglutinates. For those RBx with very little or no glassy matrix, positive classification rests on the identification of some regolith component in thin section.

Monomict breccias and igneous rocks. Aproximately 30 particles are classified as igneous or "mostly monomict" on the basis of petrographic features and low siderophile-element concentrations. Although some of these may not be strictly pristine, they retain compositions and petrographic features dominated by a single igneous lithology. These are of particular interest because igneous rocks are rare among Apollo 14 samples; any samples that may better characterize or extend the suite of Apollo 14 igneous rocks are valuable. Specific lithologic classifications and compositions of these particles are given in Table 5, and REE patterns are plotted in Fig. 5.

Several particles have anorthositic compositions and consist dominantly of aggregates of plagioclase crystals (Fig. 2i); some consist partly or wholly of glass or partially devitrified glass. The crystalline particles and crystalline patches of glassy particles have uniform mineral compositions, as indicated by electron microprobe analyses. One particle has the bulk composition of alkali anorthosite, and three others have compositions dominated by alkali anorthosite or alkali noritic anorthosite. These are characteristically enriched in Na and Eu (cf. *Warren and Wasson,* 1980; *Warren et al.,* 1983a,b, 1987; *Shervais et al.,* 1984). Only one particle has a composition similar to that of previously reported magnesian-suite anorthosite (cf. *Shervais et al.,* 1983, 1984; *Lindstrom et al.,* 1984). This particle has magnesian, high-Ca pyroxene [Mg/(Fe + Mg): 0.91] and anorthitic plagioclase (An_{96}) (Fig. 6). Three particles have the composition of ferroan anorthosite, which is very rare among previously characterized Apollo 14 materials (*Shervais,* 1989; *Warren et al.,* 1983a). Two of these are crystalline and one is partly glassy. One of the crystalline fragments (,7033) has mineral compositions that are consistent with its classification as ferroan anorthosite and one (,7237) has slightly more magnesian pyroxene than typical, but is not sufficiently magnesian to belong to the Mg-suite (Fig. 6).

Several particles appear to be fragments of norite (Fig. 2j) or gabbronorite, although in some cases coarse grain size precludes a representative modal determination. Mineral compositions are uniform within these fragments, so the modal determinations are based on comparisons of modal recombinations to bulk compositions determined by INAA, as well as on point counts of thin sections. Compositions of minerals in the norite and gabbronorite particles that are included in Table 5 indicate that these particles are mainly fragments of Mg-suite lithologies (Fig. 6). Gabbronorite 14161,7044 has

TABLE 4. Regolith breccias and agglutinates.

Specific	INAA	Na_2O	CaO	Sc	Cr	FeO	Co	Ni	Zr	Cs	Ba	La	Sm	Specific
,7067	212.087	0.73	11.5	20.0	1330	9.42	30.9	280	910	0.7	770	60.5	27.0	,7067
,7115	216.015	0.70	10.8	20.6	1301	9.81	30.6	<370	680	1.0	740	62.0	27.8	,7067
,7274	219.113	0.67	11.6	22.4	1407	10.72	36.4	<400	1010	0.7	750	61.2	28.0	,7274
,7249	219.088	0.66	11.4	21.4	1321	10.07	33.9	310	890	1.0	780	62.9	28.6	,7249
,7162	216.071	0.68	11.0	21.3	1350	10.08	35.8	300	1190	0.6	730	64.2	28.9	,7162
,7253	219.092	0.64	9.0	21.6	1405	10.32	36.1	330	970	0.6	748	64.0	29.2	,7253
,7097	212.117	0.67	9.5	21.1	1320	10.01	33.6	280	1100	0.5	870	65.7	29.6	,7097
,7224	219.050	0.64	12.0	22.4	1390	10.68	37.7	460	940	0.7	804	64.7	30.0	,7224
,7220	219.046	0.67	10.9	23.2	1467	10.88	35.6	337	1050	0.6	784	64.9	30.0	,7220
,7112	216.012	0.68	11.0	21.7	1370	10.36	33.8	350	1100	0.9	770	67.4	30.1	,7112
,7101	216.001	0.66	11.6	21.8	1390	10.45	37.3	380	980	0.6	800	66.8	30.2	,7101
,7193	219.019	0.67	10.9	21.7	1354	10.40	35.1	300	1190	0.7	830	65.6	30.3	,7193
,7189	219.015	0.67	11.8	22.0	1380	10.53	37.7	420	1120	1.2	790	65.4	30.3	,7189
,7065	212.085	0.73	10.0	23.4	1410	10.77	33.8	270	860	0.8	800	69.0	30.3	,7065
,7117	216.017	0.73	12.5	22.0	1360	10.55	34.5	<dl	950	1.1	920	68.7	30.5	,7117
,7146	216.055	0.87	12.0	20.6	1255	9.51	28.3	260	1040	0.7	920	68.9	30.5	,7146
,7198	219.024	0.64	11.1	22.2	1387	10.54	35.8	321	977	0.7	773	67.1	30.6	,7198
,7272	219.111	0.71	10.5	21.4	1348	9.94	29.8	290	980	0.7	840	67.8	30.8	,7272
,7140	216.049	0.88	11.3	20.7	1680	9.73	27.7	240	810	0.7	870	70.5	30.8	,7140
,7252	219.091	0.74	10.0	21.7	1350	10.31	36.0	450	1010	0.8	870	68.6	30.9	,7252
,7119	216.019	0.73	10.5	21.7	1393	11.16	55.2	810	1010	0.7	820	69.3	31.5	,7119
,7003	212.013	0.75	10.2	23.0	1372	10.75	34.9	360	1020	0.7	850	70.9	31.6	,7003
,7103	216.003	0.87	9.9	21.2	1290	9.91	30.1	<500	1440	1.0	870	75.6	33.6	,7103
,7183	219.009	0.92	9.1	16.8	1212	9.05	30.3	340	1190	1.7	1080	83.7	35.4	,7183
,7017	212.027	0.91	10.7	19.8	1250	9.94	30.1	220	1020	1.1	900	80.8	36.9	,7017
,7026	212.036	0.87	12.2	17.3	989	8.22	20.2	230	1260	1.8	1420	87.9	38.1	,7026

TABLE 4. (continued).

Specific	Eu	Tb	Yb	Lu	Hf	Ta	Ir	Au	Th	U	Mass	Description	Specific
,7067	2.17	5.5	19.6	2.71	21.5	2.9	<13	6	11.7	3.4	18.1	RBx	,7067
,7115	2.30	5.7	20.0	2.73	21.8	2.4	<30	5	10.9	3.3	48.3	RBx	,7115
,7274	2.60	5.6	20.0	2.75	22.7	2.6	18	10.1	11.1	3.3	28.8	RBx	,7274
,7249	2.20	5.5	20.4	2.78	21.3	2.8	<25	7	12.3	3.4	33.9	RBx	,7249
,7162	2.26	5.6	21.0	2.84	23.0	3.1	12	4.5	12.4	3.3	21.9	RBx	,7162
,7253	2.42	5.8	20.8	2.85	23.1	3.0	11.8	8.1	12.3	3.5	23.8	RBx-Agg	,7253
,7097	2.25	6.0	21.4	2.91	22.8	3.0	<23	<8	12.8	3.1	19.7	RBx	,7097
,7224	2.53	5.9	22.0	2.96	24.0	3.1	15.3	<9	12.6	3.3	28.9	RBx-Agg	,7224
,7220	2.51	5.9	22.0	2.99	25.3	3.1	10.9	7.8	12.5	3.4	32.7	RBx-Agg	,7220
,7112	2.60	6.0	21.7	2.93	23.7	2.5	<27	<11	13.0	3.5	47.7	RBx	,7112
,7101	2.44	5.8	21.6	2.95	23.9	2.9	13	7	12.7	3.6	41.8	RBx-Agg	,7101
,7193	2.36	5.9	22.3	3.02	24.2	3.0	16	5.5	13.3	3.7	46.8	RBx	,7193
,7189	2.60	5.7	22.0	2.96	23.8	3.2	<23	5.1	12.9	3.3	36.6	RBx-Agg	,7189
,7065	2.40	6.2	22.7	3.14	23.3	3.0	16	5	13.7	3.6	12.8	RBx	,7065
,7117	2.70	5.9	21.7	3.01	24.1	2.7	<32	<8	13.7	3.9	56.6	RBx	,7117
,7146	3.14	6.0	21.8	3.05	23.5	3.0	9	8	12.7	3.2	27.1	RBx	,7146
,7198	2.49	6.1	22.0	2.99	23.3	3.1	11.9	4.7	13.1	3.6	35.8	RBx-Agg	,7198
,7272	2.31	6.1	22.0	2.92	22.9	2.6	<dl	4.5	13.4	3.5	24.0	RBx	,7272
,7140	3.00	6.2	22.7	3.06	23.9	2.8	12	6	12.7	3.6	29.3	RBx	,7140
,7252	3.04	6.5	22.2	3.03	23.6	3.1	<30	7	12.8	4.0	32.6	RBx	,7252
,7119	2.57	6.2	22.2	3.02	24.0	2.8	36	10	12.8	4.0	44.0	RBx-Agg	,7119
,7003	2.67	6.4	23.4	3.18	23.8	3.2	11.8	<9	13.7	3.7	13.6	RBx	,7003
,7103	2.50	6.4	24.5	3.27	26.6	3.0	<28	<12	14.3	4.2	44.1	RBx-Agg	,7103
,7183	2.65	7.1	31.2	4.30	27.4	5.4	<dl	8.5	27.0	7.2	34.3	RBx	,7183
,7017	2.60	7.4	26.0	3.58	25.8	3.6	<24	6	16.0	4.0	11.3	RBx	,7017
,7026	2.59	7.7	28.4	3.94	29.4	3.7	<10	<5	18.9	5.4	13.2	RBx	,7026

Na_2O, CaO, and FeO in % (cg/g, total element as oxide); Au and Ir in ppb (ng/g); all other values in ppm (μg/g). "<dl" = below detection limit (no concentration value obtained) and no upper limit estimate made. Uncertainties are given in section on Analytical Procedures. RBx: regolith breccia, fragmental or glassy matrix; RBx-Agg: partially fused soil or large agglutinate.

TABLE 5. Igneous fragments (mostly monomict) from 14161.

Specific	INAA	Na_2O	CaO	Sc	Cr	FeO	Co	Ni	Zr	Cs	Ba	La	Sm	Specific
,7033	212.043	0.34	19.1	2.11	99	0.75	1.0	11	<19	0.02	17	1.03	0.48	,7033
,7236	219.075	0.37	17.9	2.70	167	1.80	3.8	<17	<30	0.03	18	1.25	0.56	,7236
,7237	219.076	0.29	18.2	4.03	455	2.28	5.1	<25	<30	0.05	13	0.64	0.25	,7237
,7350	231.078	0.58	16.9	1.28	78	0.99	5.1	20	<dl	0.08	440	95.4	44.3	,7350
,7128	216.037	1.41	13.8	12.7	468	5.72	10.6	65	850	0.46	1000	72.1	29.8	,7128
,7229	219.055	1.12	14.8	13.0	876	5.11	9.3	34	555	0.26	591	46.3	20.2	,7229
,7245	219.084	1.74	17.7	4.57	110	1.87	8.4	42	527	0.11	600	59.6	23.9	,7245
,7312	231.031	1.60	14.8	4.43	268	2.04	6.2	50	201	0.19	540	23.4	7.91	,7312
,7076	212.096	0.68	13.4	21.3	1413	6.83	18.2	82	590	0.53	725	34.0	17.4	,7076
,7037	212.047	0.68	7.2	19.2	1950	9.60	22.3	<80	260	0.24	323	11.2	3.72	,7037
,7044	212.054	0.77	11.6	18.2	1176	8.99	13.7	<90	580	0.57	670	119	55.5	,7044
,7080	212.100	0.51	9.0	17.1	1600	9.21	16.1	145	85	0.13	239	33.6	15.2	,7080
,7207	219.033	0.72	13.0	20.0	1101	8.93	17.0	<230	1110	0.8	721	67.8	29.6	,7207
,7048	212.058	0.70	15.0	15.5	919	6.72	11.3	43	740	0.51	573	48.9	21.3	,7048
,7062	212.082	0.69	10.9	16.4	984	7.24	11.2	68	760	0.57	599	49.1	21.7	,7062
,7066	212.086	0.67	11.4	15.4	932	6.73	12.8	39	660	0.43	522	43.5	19.4	,7066
,7110	216.010	0.76	12.1	18.4	1140	8.14	13.7	<80	800	0.51	570	51.4	22.6	,7110
,7069	212.089	1.41	9.0	30.2	361	13.99	7.2	<110	4240	1.6	2050	228	96.5	,7069
,7373	231.101	0.75	11.3	42.2	982	16.05	15.0	<100	7150	0.36	740	696	326	,7373
,7269	219.108	0.71	7.5	15.6	680	7.40	15.1	106	1240	5.0	2290	95.3	35.6	,7269
,7064	212.084	0.54	12.0	58.2	3270	12.46	26.8	170	270	1.2	500	17.0	9.6	,7064

TABLE 5. (continued).

Specific	Eu	Tb	Yb	Lu	Hf	Ta	Ir	Au	Th	U	Mass	Description	Specific
,7033	0.82	0.10	0.33	0.043	0.26	0.03	<dl	<0.6	0.15	0.03	21.1	Fer Anor	,7033
,7236	0.73	0.08	0.31	0.042	0.26	0.06	<dl	<1.7	0.12	<0.08	40.4	FA Gl	,7236
,7237	0.71	0.04	0.17	0.023	0.09	0.02	<dl	<dl	0.04	<dl	29.2	Fer Anor	,7237
,7350	3.22	7.1	15.3	1.82	1.19	0.03	<9	<4.2	4.14	<0.25	11.8	Mg Anor	,7350
,7128	5.48	6.1	23.6	3.29	20.6	2.9	<3.2	<4	13.7	3.9	27.2	AA + Gl	,7128
,7229	4.50	3.9	14.2	1.96	14.0	2.1	<2.9	<dl	6.7	1.9	63.1	AA + Gl	,7229
,7245	6.91	4.4	13.3	1.74	12.7	1.4	<dl	<5	6.5	1.9	40.8	AA Bx	,7245
,7312	6.40	1.44	5.39	0.735	4.77	0.71	3.3	<3.6	3.0	0.9	10.1	AA + Gl	,7312
,7076	1.97	4.2	19.6	2.68	15.6	2.3	<dl	<2.3	8.6	3.1	10.3	Gab-nor	,7076
,7037	2.06	0.94	7.8	1.21	7.4	0.53	<dl	<4	2.3	1.1	20.7	Norite	,7037
,7044	2.61	10.9	31.2	4.09	15.4	2.4	<dl	<dl	14.7	3.0	17.9	Gab-nor	,7044
,7080	1.85	2.85	9.0	1.23	2.67	0.19	2.4	<5	5.2	1.0	15.6	Norite	,7080
,7207	2.17	6.0	21.8	3.01	25.5	3.1	<dl	<6	13.8	4.0	58.8	KREEP Bas	,7207
,7048	2.15	4.4	15.4	2.12	17.0	2.0	<dl	<4	9.7	2.5	20.3	KREEP Bas	,7048
,7062	2.01	4.3	16.2	2.27	18.3	2.2	<3	<5	10.3	2.9	25.7	KREEP Bas	,7062
,7066	1.89	3.9	14.3	1.96	15.6	1.9	2.3	<3	8.5	2.2	28.4	KREEP Bas	,7066
,7110	1.94	4.6	16.7	2.24	18.6	2.2	<dl	<5	10.0	2.9	85.3	KREEP Bas	,7110
,7069	3.35	20	74	10.2	100	9.2	<dl	<dl	44	12.2	22.9	QMD	,7069
,7373	5.68	62	146	18.7	163	4.3	<dl	<dl	37	5.4	18.4	W-QMD	,7373
,7269	2.69	8.5	55.3	7.9	32.8	11.0	<6	<4	66	20	36.4	Felsite	,7269
,7064	1.55	2.31	9.2	1.24	5.03	0.95	<dl	<6	2.8	1.14	19.6	VHK MBas	,7064

Na_2O, CaO, and FeO values are in % (cg/g, total element as oxide); Au and Ir values are in ppb (ng/g); all other values are in ppm (μg/g). "<dl" = no concentration value obtained and no upper limit estimate made. Analytical uncertainties: 1-2%—Na_2O, Sc, Cr, Fe, Co, La, Sm, Eu, Tb, Yb, Lu, Hf, Th; 5-6%—CaO, Ba, Ta; 10-15%—Zr, Cs, U; 15-25%—Ni, Ir, Au. FA: ferroan anorthosite; AA: alkali anorthosite (Gl: glass; Bx: breccia); Gab-nor: gabbronorite. KREEP Bas: LKFM-IKFM KREEP basalt, no clasts; VHK MBas: very-high-K mare basalt; QMD: quartz monzodiorite (W: whitlockite).

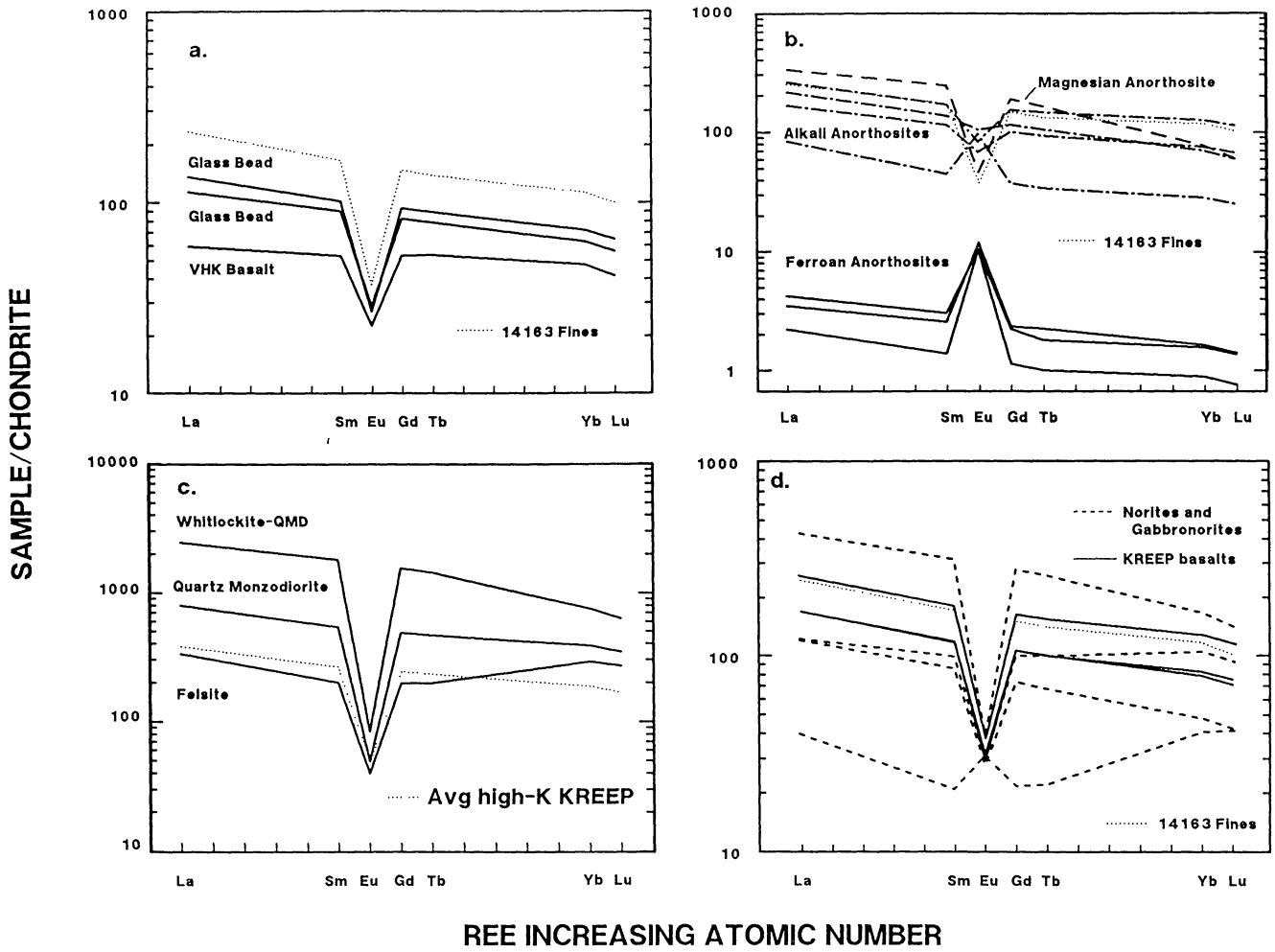

Fig. 5. Chondrite-normalized REE concentrations in "mostly monomict" particles from 14161: **(a)** basalt and basaltic glass, **(b)** alkali, magnesian, and ferroan anorthosite, **(c)** QMD and felsite, **(d)** norite, gabbronorite, and KREEP basalt.

high REE concentrations (119 ppm La) that might suggest contamination or metasomatic alteration by KREEP-rich liquid; however, this particle is not uniformly enriched in ITEs (La/Yb greater than that of KREEP; concentrations of ITEs other than REE much less than those of KREEP). It contains relatively coarse-grained phosphates and may be part of a phosphate-bearing cumulate. Chondrite-normalized REE patterns of these particles are shown in Fig. 5d.

Several particles are classified as KREEP basalts in Table 5. Their compositions are similar to that of 14310 (*Hubbard et al.,* 1972; *Haskin et al.,* 1973) and 14276 (*Brunfelt et al.,* 1972), but bulk Ni concentrations are only 0.2-0.5 times as high and Ni/Co values are relatively low (<100 ppm Ni and Ni/Co of 4-6). These have coarsely crystalline, subophitic to intersertal textures, contain no obvious clasts, and are only weakly shocked (Fig. 2k). They contain some 50 wt% plagioclase and 45% pyroxene as major minerals. *Ryder* (1987) advocated criteria such as homogeneous igneous textures, cotectic compositions, lack of clasts, absence of meteoritic siderophile-element concentrations, and the presence of phenocrysts, indicative of nonlinear cooling, as evidence of an endogenous origin for Apollo 15 KREEP basalts. With the exception of strictly cotectic compositions and siderophile element data that are ambiguous, these criteria are met for several of the Apollo 14 KREEP basalt fragments we have found. *Ryder et al.* (1980) advocated direct analyses of metal fragments to test for meteoritic contamination. Preliminary electron microprobe analyses of metal in the 2-4-mm fragments also yield ambiguous results (<8% Ni and Ni/Co: 2-9), not definitively pristine, but some analyses are outside the range for 14078 KREEP basalt (Ni ~4-22%, Ni/Co ~6-15) and near the range for Apollo 15 KREEP basalts (Ni <1%, Ni/

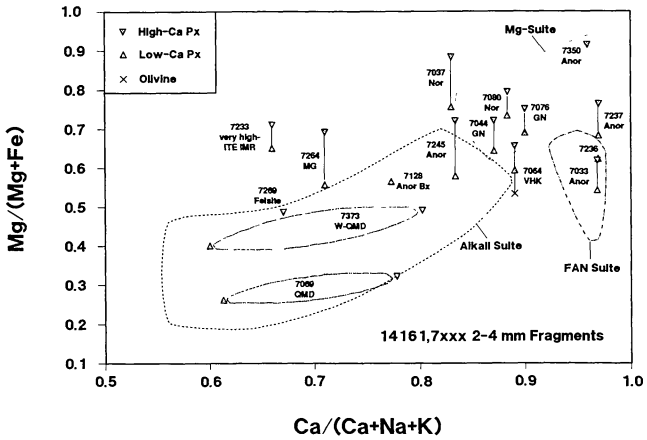

Fig. 6. Plot of Mg/(Mg+Fe) in mafic silicates vs. An content of coexisting plagioclase in selected particles from 14161. Fields for Mg-suite, FAN-suite, and alkali-suite rocks based on many literature references. Fields for QMD fragments are drawn to include the range of compositions observed in their plagioclase. MG = monzogabbro, GN = gabbronorite.

Co ~0.7-2.5) shown by *McKay et al.* (1978). The petrology of these fragments and their relationship to impact-derived Apollo 14 KREEP basalts and to Apollo 15 volcanic KREEP basalts will be deferred to a subsequent paper, but for the purpose of this paper, these fragments are considered to be monomict.

Three of the particles are fragments of compositionally evolved felsite (fine-grained granite) and quartz monzodiorite (QMD). One particle is a shocked and partially recrystallized fragment of QMD that is compositionally and petrographically similar to 15405,51 and 15459,315 (*Taylor et al.,* 1980; *Lindstrom et al.,* 1988). It has high ITE concentrations and KREEP-like concentration ratios for all ITE. Another fragment of QMD is coarsely crystalline, whitlockite-rich, and appears to be a plutonic cumulate. This fragment is compositionally and petrographically different from any previously reported lunar sample. It has the highest measured REE concentrations of any lunar rock (Fig. 5c), but it is not uniformly enriched in all ITE in KREEP-like concentration ratios (e.g., La/Yb = 4.8 vs. ~3.1 for KREEP; see also *Jolliff,* 1991). The third fragment is a mixture of glass of felsic composition, crystalline granitic clasts, and clasts of a magnesian lithology. The materials of granitic composition are very similar to those of felsite clasts from 73215 (*James and Hammerstrom,* 1977). The bulk composition (particularly the trace elements) of this particle is dominated by the materials of granitic composition, so this is listed with the "mostly monomict" particles in Table 5, and the term "felsite" is used in keeping with the usage of James and Hammerstrom. The QMD and felsite particles appear to represent petrogenetically related lithologies (cf. *Ryder,* 1976) and are described in detail elsewhere (*Jolliff,* 1990, 1991).

Several lithologies found as abundant clasts in large Apollo 14 breccia samples are absent or poorly represented among the monomict group. For example, only one particle has the composition and texture of a very-high-K (VHK) mare basalt (Fig. 5a, Table 5), and two are glass beads with mare-basalt compositions, presumably of impact origin, based on elevated siderophile element concentrations (Table 2). This is in contrast with the apparent abundance of aluminous basalt clasts in Apollo 14 breccias (*Warner et al.,* 1980; *Dickinson et al.,* 1984; *Shervais et al.,* 1985a,b; *Goodrich et al.,* 1986; *Neal et al.,* 1988), although others have noted their paucity in Apollo 14 soils (*Quaide and Wrigley,* 1972). There are only a few particles of alkali and magnesian anorthosites, and no particles of coarse-grained troctolite. We have found no particles with the compositions of pyroxenite or dunite (cf. *Warren et al.,* 1987; *Shervais et al.,* 1984; *Lindstrom et al.,* 1984).

Compositional Systematics

Concentrations of FeO and CaO are plotted in Fig. 7 to illustrate the general relationship of composition to particle type for the entire suite of particles. Iron oxide is chosen to represent the proportions of mafic minerals and CaO, as a rough indicator of high proportions of plagioclase (since we do not have data for Al). Also shown are fields for approximately 300 previous analyses of Apollo 14 samples, broadly categorized as highlands monomict rocks or clasts; soils and

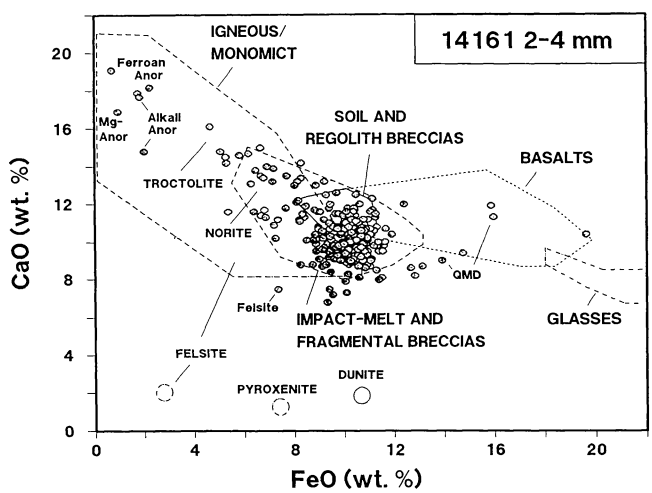

Fig. 7. Plot of CaO vs. FeO concentrations for 381 2-4-mm particles from 14161. Compositional fields are shown for 300 previous analyses of Apollo 14 materials: highlands monomict rocks or clasts; soils and regolith breccias; undifferentiated breccias, breccia matrix, and melt rocks; basalts; and glasses that do not plot in the breccia field. The approximate positions of previously reported Apollo 14 felsite, pyroxenite, and dunite are also indicated. References for catalog data: *Brunfelt et al.* (1972); *Dickinson et al.* (1984); *Goodrich et al.* (1986); *Haskin et al.* (1973); *Helmke et al.* (1972); *Hubbard et al.* (1972); *Jerde et al.* (1987); *Laul et al.* (1972); *Lindstrom et al.* (1972, 1984); *McKay et al.* (1978, 1979); *Neal et al.* (1988); *Rose et al.* (1972); *Shervais et al.* (1984, 1985a,b); *Taylor et al.* (1972); *Wänke et al.* (1972); *Warner et al.* (1980); *Warren and Wasson* (1980); *Warren et al.* (1981, 1983a,b,c, 1986, 1987).

regolith breccias; fragmental breccias, breccia matrix, and melt rocks; basalts; and mafic and ultramafic glasses. Compositions of most particles cluster in the soil and regolith breccia area of this plot. Impact-melt breccias, the most abundant group in the 2-4-mm range, have, on average, lower CaO concentrations and form a broader distribution than the regolith breccias. Only three particles have basaltic affinity—one VHK (aluminous) basalt fragment and two intermediate-Fe to Fe-rich basaltic glass beads. Several particles have anorthositic compositions and several have troctolitic to noritic compositions. Unusual compositions represented by one or several particles each include alkali anorthosite, felsite, and QMD.

The plot of Na_2O vs. La (Fig. 8) separates alkali-rich from alkali-poor particles, particularly alkali anorthosite from Mg-suite anorthosite or ferroan anorthosite. Two previously reported REE-rich anorthosite samples are also plotted in Fig. 8: alkali anorthosite 14305,283 (*Warren et al.,* 1983b), and Mg-suite anorthosite 14321,1211 (*Lindstrom et al.,* 1984). These two anorthosites show the effect of modal enrichment in whitlockite and therefore high REE concentrations, but not similar enrichments of other ITE (Cs, Ba, Zr, Hf, Ta, Th, U) relative to average high-K KREEP. Of the 2-4-mm particles from 14161, an impact-melt rock, two fragments with the composition of QMD (one a fragmental breccia), and the whitlockite-QMD plot at high La concentrations. The QMD and IMR fragments are uniformly enriched in all other ITE as well as the REE. A large proportion of the 2-4-mm particles have about 70 ppm La and 0.7 wt% Na_2O, similar to the <1-mm fines (14163). Impact-melt lithologies and a few of the fragmental breccias form a broader distribution extending to higher concentrations of both La and Na_2O than found for regolith breccias and agglutinates.

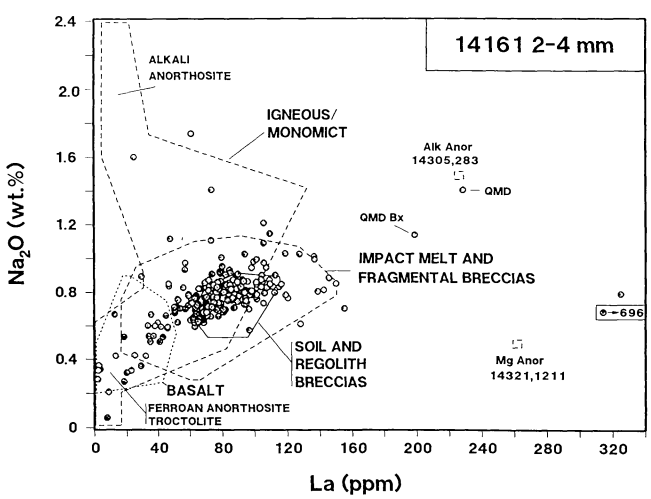

Fig. 8. Plot of Na_2O vs. La concentrations for 380 2-4-mm particles from 14161. Data references are same as for Fig. 7. Analyses of 14305,283 and 14321,1211 are given in *Warren et al.* (1983b) and *Lindstrom et al.* (1984), respectively.

Correlations among ITE concentrations are high for the entire suite of particles, as shown in Fig. 9 for the elements Sm, Yb, Ba, Th, Hf, and Ta plotted against La. Analyses of these particles were done under essentially identical conditions and analytical precision is very high, as demonstrated by the La-Sm plot (Fig. 9a). All particles have nearly the same La/Sm ratio, so the regression line extrapolates to the origin. The correlation between La and Yb is also very high (correlation coefficient: 0.95), but the regression line (determined with or without outliers) does not extrapolate to the origin (Figs. 9b and 10), indicating that, along the regression line, fragments with low REE concentrations have higher Yb/La than fragments with high REE concentrations. There appears to be a slight break in slope at about 40 ppm La. At La concentrations less than 40 ppm, compositions of polymict particles fall along a trend toward the origin, forming an "apparent" mixing line with the compositions of ferroan anorthosite particles. (This apparent mixing trend does not hold for compatible trace elements, e.g., Sc, as shown below.) If we assume that there is an igneous lithology (or group of lithologies that, as a mixture, form an endmember component) with low ITE concentrations (~ 40 ppm La), then it has a higher Yb/La ratio than the component or components with high ITE concentrations. A simple mixing scenario with only two main components cannot explain the bulk compositions of the polymict particles with La > 40 ppm, because concentrations for so many elements are not mutually correlated (e.g., La-Sc, Fig. 11). This is discussed in more detail below. Of all 381 particles, only the felsite fragment consistently deviates from the regression lines against La. Other notable deviations from regression lines in Fig. 7 occur for the anorthosite fragments (ferroan and magnesian suite) and the QMD fragments.

The monomict, apparently igneous particles among the 2-4-mm particles have counterparts among the igneous rock types previously reported. Lanthanum and Yb concentrations in Apollo 14 igneous materials taken from both the literature and this work are plotted in Fig. 12. The extrapolation of the regression line from Fig. 10 is also shown on this diagram. Alkali-suite and Mg-suite anorthosites with high REE concentrations have low Yb/La and lie along a trajectory toward whitlockite. The basalt field, mainly based on clasts from 14321, has a positive intercept and high Yb/La. The norite field, which includes gabbroic norite and Apollo 14 KREEP basalt, also lies along the extrapolated regression line.

The correlations between pairs of ITEs, particularly REE, Hf, Zr, Th, U, and Ta, are remarkably tight, as discussed above, despite petrographic differences and diversity in major-element concentrations of the polymict 2-4-mm particles. However, correlations between La and Zr, Hf, Th, or Ba concentrations are not as high as those between La and the other REE (Figs. 9c,d). This reflects real modal variations among the phosphates (which host the bulk of the REE), zircon (Zr, Hf), and K-feldspar (Ba), although the positive correlations indicate the broad coherence of these minerals in the ITE-bearing components. On the La-Ba plot, the scatter from the main trend toward high Ba/La might suggest the presence of as much as 40% of a granitic component in some of the polymict particles; however, this degree of scatter is not present for the same particles in the plots of La vs. Yb, Th, and Ta, which are

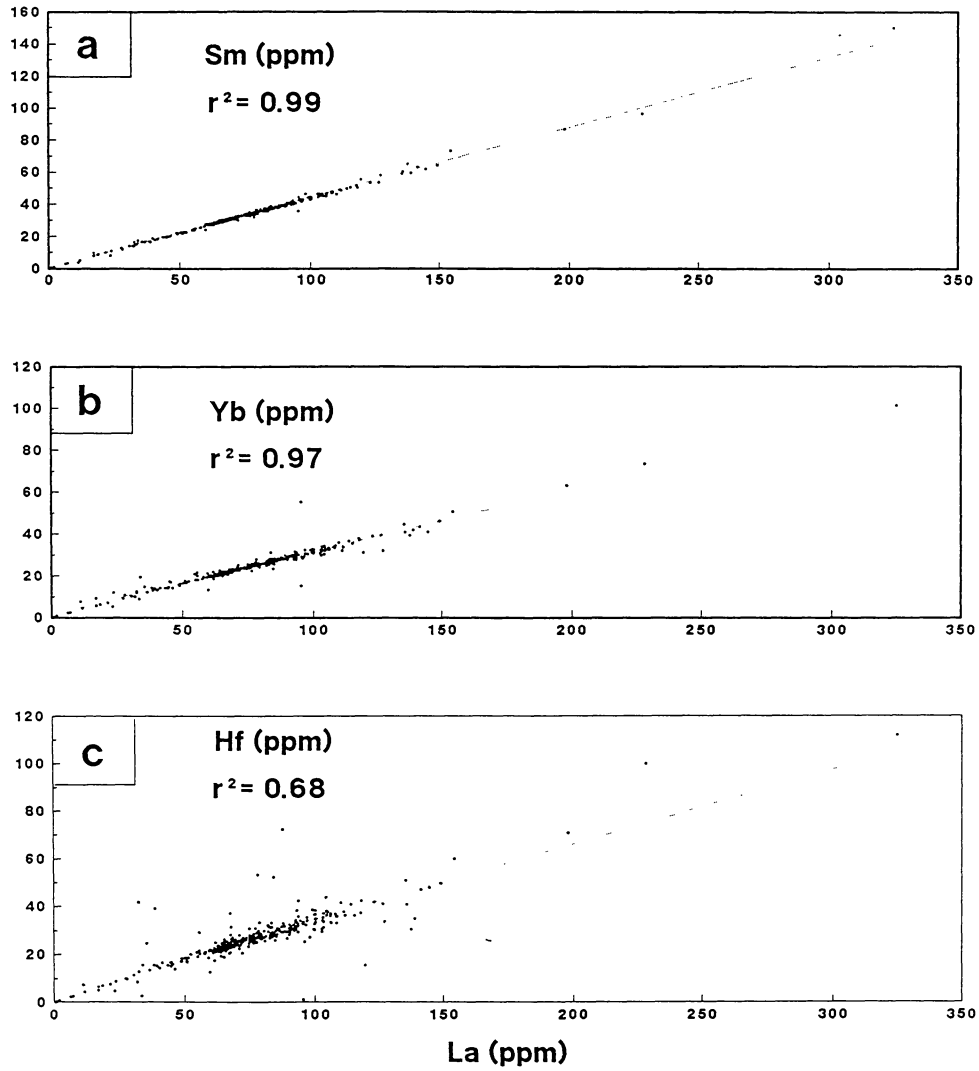

Fig. 9. Incompatible element concentrations plotted against La concentrations in 2-4-mm particles from 14161, excluding the whitlockite-rich QMD (700 ppm La): **(a)** La vs. Sm; **(b)** La vs. Yb; **(c)** La vs. Hf; **(d)** La vs. Ba; **(e)** La vs. Th; **(f)** La vs. Ta. The correlation coefficients (given as r^2) and regression lines are based on the compositions of the polymict particles.

also diagnostic for lunar granite. Therefore, a granitic component, although possibly present as clasts in the polymict particles, is not the cause of most of the scatter on the La-Ba plot. Instead, we attribute the scatter to variations in the modal abundance of K-feldspar.

DISCUSSION

Lithologic Distribution of 2-4-mm Particles

By analyzing a large number of particles without any petrographic preselection criteria, we have obtained the proportions of compositionally different particle types in this sample of 2-4-mm particles. If the igneous rock types found as clasts in the larger breccia samples have contributed volumetrically significant proportions of the material that now makes up the soils, we might expect to find fragments of them among the soil fragments. It is evident in Fig. 7 (CaO vs. FeO), however, that the soil fragments do not cover the entire range of compositions of known Apollo 14 rock types and that certain igneous lithologies are not as abundant as we might have expected from breccia pull-apart studies. We emphasize that the sampling of breccias typically is not random; instead, the igneous or unusual clasts are deliberately sought. We find very few fragments of aluminous or VHK mare basalts, alkali anorthosite, troctolite, felsite, and dunite. Others have also noted that basaltic particles are rare among the soil fragments (*Engelhardt et al.,* 1972; *Quaide and Wrigley,* 1972; *McKay et al.,* 1972; *Powell and Weiblen,* 1972; *Simon et al.,* 1982). This suggests that the large breccias, many of which were ejected from Cone Crater, derive from a different or additional portion of bedrock than the Apollo 14 surface soils.

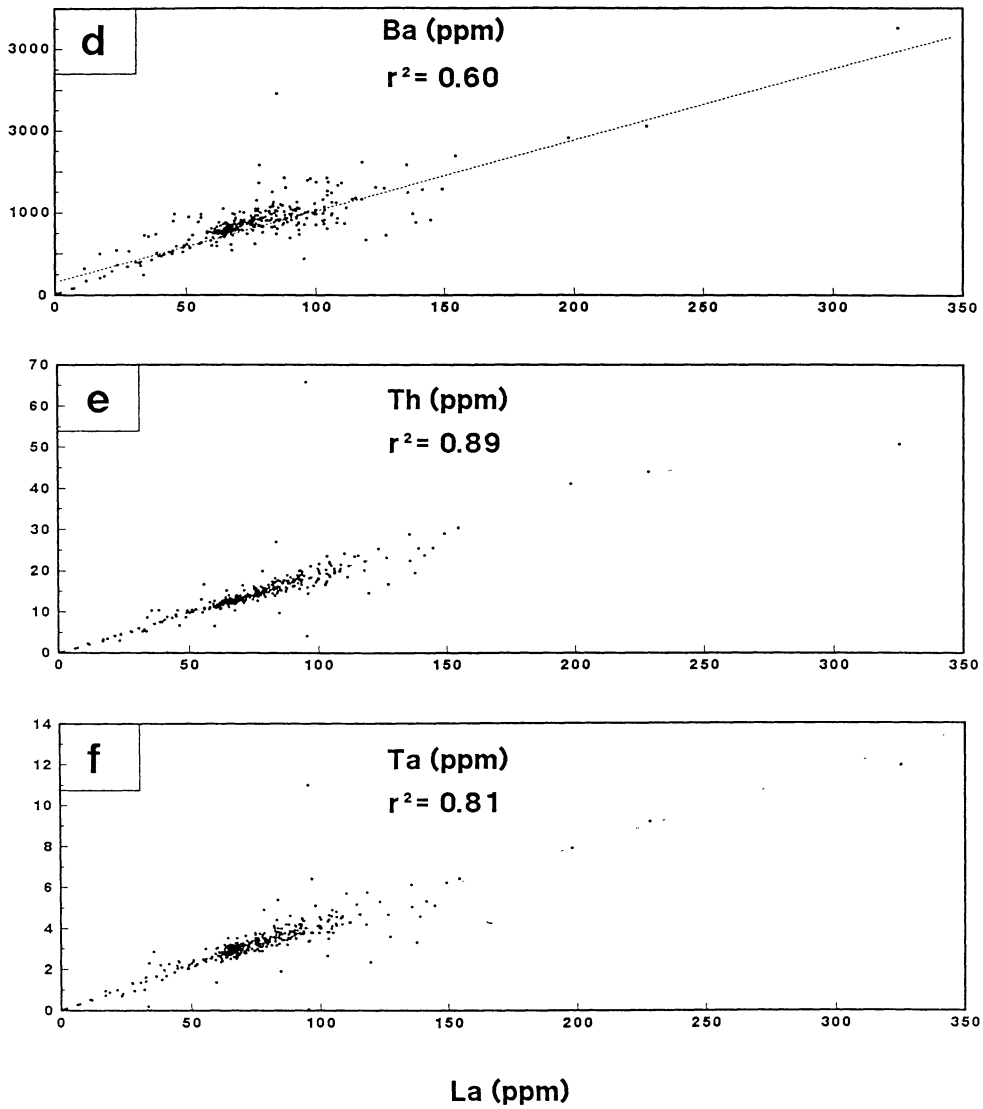

Fig. 9. (continued).

There are no significant compositional differences between the <1-mm fine soil at the LM site (e.g., 14163) and the fine soil from the rim of Cone Crater, based on previous analyses of 14141 (*Lindstrom et al.,* 1972; *Laul et al.,* 1982) and on our analyses (Table 6), except that siderophile-element concentrations are significantly lower and Na concentrations higher in 14141 compared to 14163. This probably results from the lower maturity of 14141, that is, less history of exposure to micrometeorites than 14163; the latter was enriched in siderophile elements by the contribution from micrometeorites and depleted in Na by volatilization. This is consistent with petrographic data on the agglutinate contents of these soils. *McKay et al.* (1972) found 20% agglutinates in 14163 compared to 1% in 14141 0.25-1-mm size fractions. *Simon et al.* (1981, 1982) found 45.7% agglutinates in 14163 and 11.7% in 14141 in the 0.09-1-mm size fractions. Among the coarse fines (1-4-mm) we find about 18% agglutinates (percent of total number of particles) in 14161 and 2.4% in 14142/3. Cone crater fines (14141) therefore appear to represent a near-surface soil that predated Cone Crater formation and was simply uncovered by the impact. The 14141 fines are in fact more similar to the 14149 trench-bottom soil than to the other Apollo 14 surface soils (*McKay et al.,* 1972; *Simon et al.,* 1982). The low Ir/Au ratio of immature soil 14141 is similar to that of the light impact-melt breccias (~1; Table 6); both ratios are subchondritic and typical of that for "ancient" impactors from Apollo 14 and 16 (*Hertogen et al.,* 1977). The Ir/Au ratio of 14163 (~2), a substantially more mature soil, is greater because it contains, in addition, a component of chondritic micrometeorites (Ir/Au = 3.4) (*Wlotzka et al.,* 1973). We conclude that the Apollo 14 surface soils, including Cone Crater soil fine 14141, differ mainly in

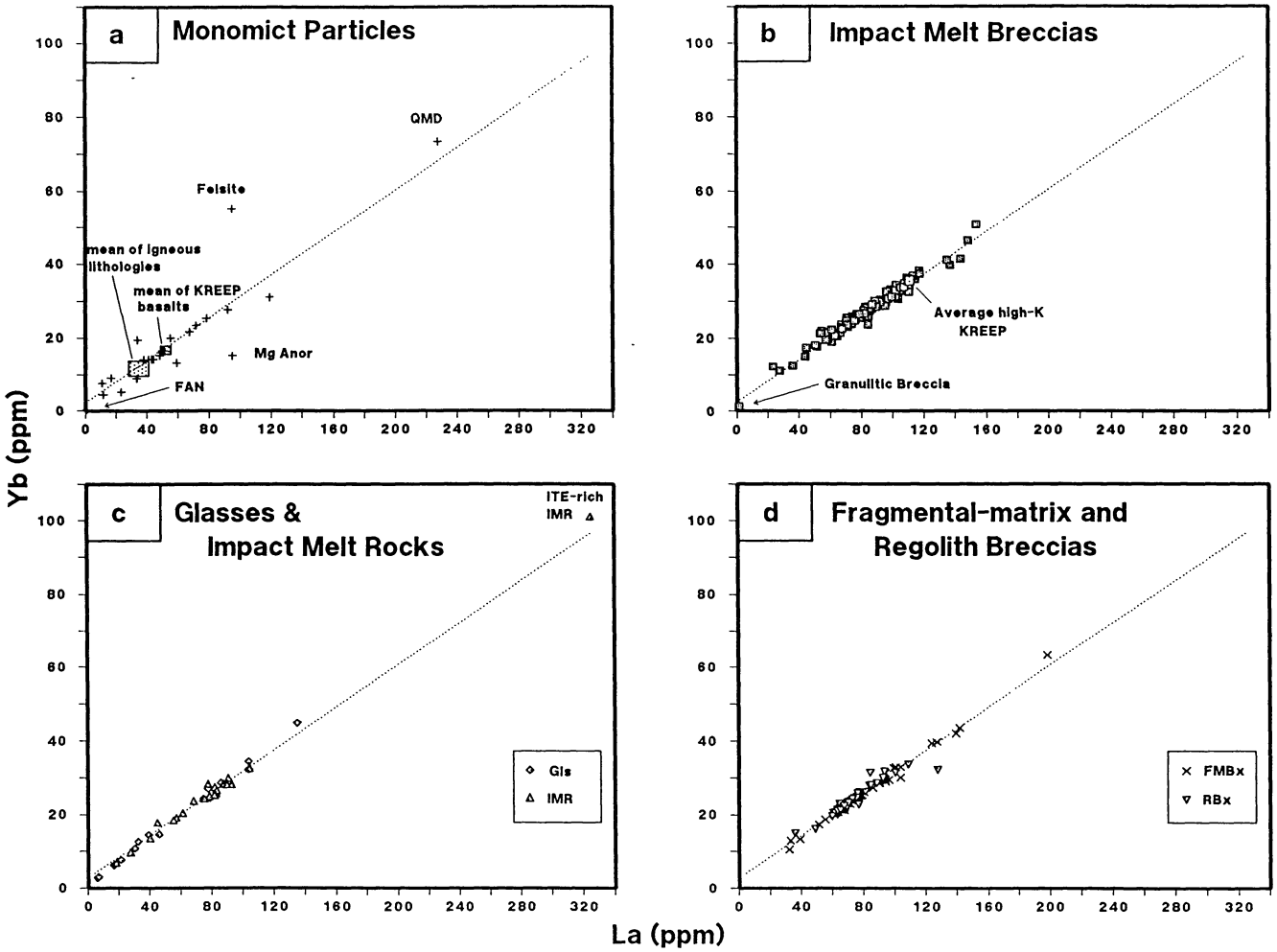

Fig. 10. Lanthanum vs. Yb concentrations for 2-4-mm particles from 14161. Line fit by least-squares regression of all particle compositions after excluding outliers. The same regression line is plotted in **(a)**, **(b)**, **(c)**, and **(d)**. The mean La and Yb concentrations of the monomict particles from 14161, excluding those with greater than 90 ppm La and excluding the KREEP basalts, plot within the stippled rectangle. The size of the rectangle represents the standard error of the mean ($\sigma/\sqrt{n}$). The smaller rectangle represents the mean of the KREEP basalt compositions. The composition of "average high-K KREEP" is from *Warren* (1989).

their exposure history, but as a group have a somewhat different provenance or an additional source of material than the large breccias ejected from Cone Crater.

Unlike the <1-mm soil fines, however, the 2-4-mm particles from the Cone Crater soil contain some of the igneous lithologies found in the Cone Crater breccias, particularly mare basalt fragments (Fig. 13). Thus the average composition of the coarse fines reflects a contribution from lithologies such as mare basalt and alkali anorthosite clasts of these breccias, particularly in FeO, Na_2O, Sc, and Cr concentrations (Table 6). *Stöffler et al.* (1986, 1989) have suggested that different large breccia samples come from two lithologically distinct levels in the underlying Fra Mauro Formation, the upper one dominated by high-K KREEP impact-melt breccias, and the lower one dominated by anorthositic lithologies of alkaline character. Thus the <1-mm fines of the surface soils have been derived mainly from the upper unit or "Apollo 14 subregolith basement" (*Stöffler et al.,* 1989) but there has been little contribution to the soil from the rocks of the deeper "megabreccia unit" that was penetrated and sampled by the formation of Cone Crater.

Relationship of 2-4-mm Particles to the Soil-forming Process

The distribution of particle types in the 2-4-mm size range and their compositions can provide information about the soil-forming process. Large agglutinates or small, glassy regolith breccias may form locally from micrometeorite impacts. We would expect constructional particles in the 2-4-mm size range developed from the <1-mm fines to have essentially the same composition as the <1-mm fines. This appears to be the case for the group A regolith breccias and agglutinates (Table 6), which are discussed in more detail below.

The 2-4-mm particles in 14161 other than the group A regolith breccias and agglutinates represent fragments of rocks that were part of impact structures (e.g., melt sheets) or were

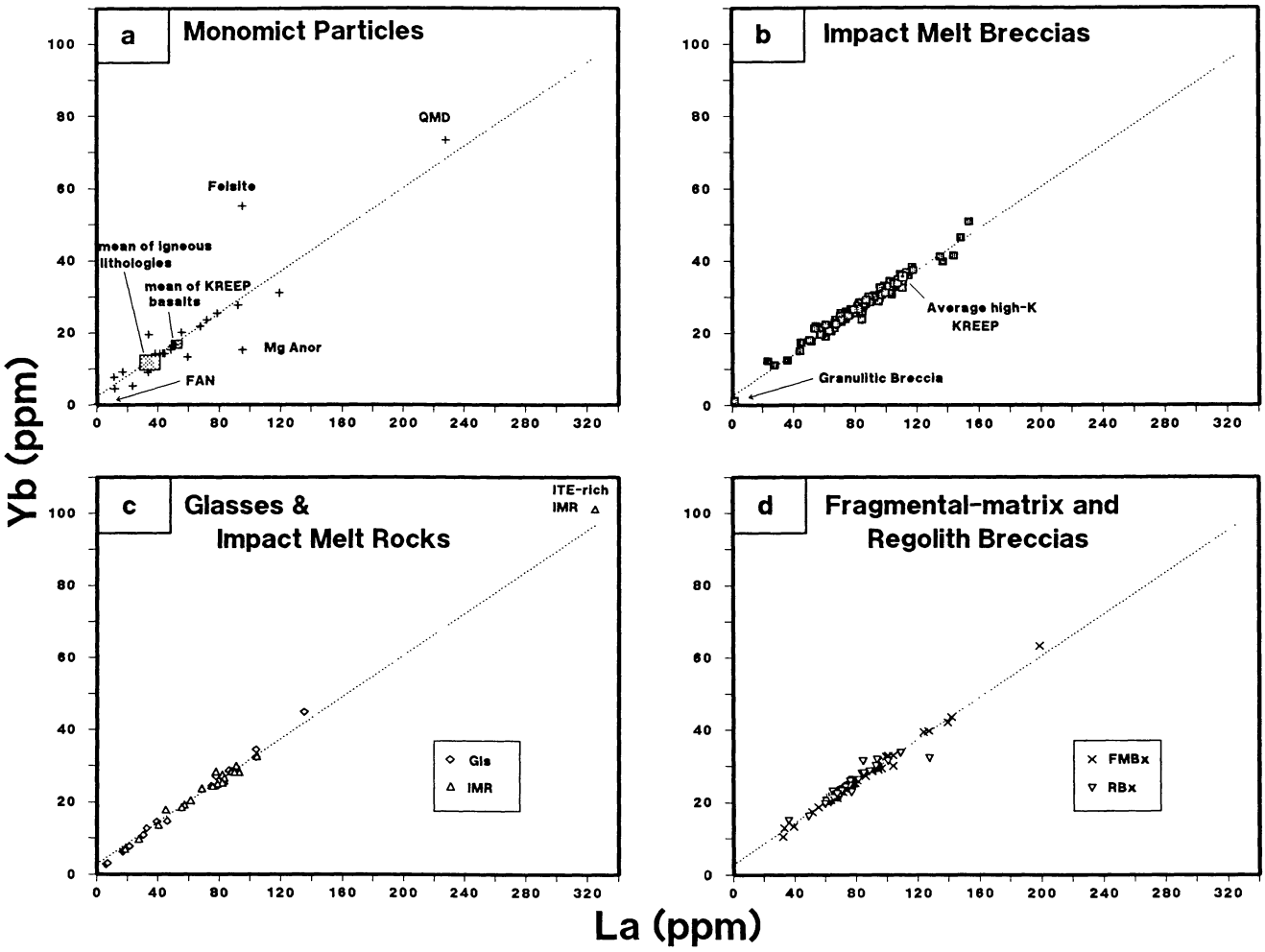

Fig. 11. Lanthanum vs. Sc concentrations of different categories of particles from 14161 (cf. Fig. 10). The mean La and Sc concentrations of the igneous particles from 14161 that have <90 ppm La plot within the larger stippled rectangle, and KREEP basalts plot within the smaller rectangle. These represent the standard error of the means and are calculated the same way as described in the caption of Fig. 10. The position of average high-K KREEP is shown for reference. The bounding lines on each figure are the same and are arbitrarily drawn to include the stippled rectangles, average high-K KREEP, QMD, and the ITE-rich impact-melt rock (c). The "monomict" particle that plots at ~30 ppm Sc and ~90 ppm La is a cataclastic gabbro whose original composition may have been modified. The average compositions of impact-melt breccias and regolith breccias are given in Table 6 and are discussed in the text.

constructed by breccia formation during impacts into these or into igneous rocks, and have not yet undergone comminution to a grain size of <1 mm. The mass-weighted mean composition of the 2-4-mm particles differs from the composition of the <1-mm fine soil 14163 in that it has higher Na_2O and ITE concentrations and lower Sc, Co, Cr, Fe, and CaO concentrations. These 2-4-mm particles cannot represent an unbiased sampling of the source materials that produced the <1-mm fines. In principle, they might represent the durable, residual portions of source rocks that survived the comminution process. We note that the <1-mm fines from 14141 and 14163 are nearly identical in lithophile-element concentrations even though their surface exposure histories are quite different. This seems to suggest that local differential comminution by micrometeorites has not been the major cause of compositional differences between the <1-mm fines (14163) and the associated 2-4-mm particles (14161). As an alternative to differential comminution, the 2-4-mm particles (or the <1-mm fines) may contain a proportion of materials that have been added to the bulk regolith since the time of emplacement of the Fra Mauro Formation. Possible examples of later additions are the volcanic glass bead components in the surface soil fines (e.g., *McKay et al.,* 1972; *Quaide and Wrigley,* 1972; *Delano,* 1988; *Simon et al.,* 1989).

Group A regolith breccias and agglutinates have essentially the same compositions as the associated <1-mm fines. This is the expected consequence if the breccias were formed from the local soil (as for bulk agglutinates; *Papike et al.,* 1981). For regolith breccia group A to have been assembled at a distant site from unrelated materials and yet have nearly the same composition as the <1-mm fines would be fortuitous. Alternatively, the <1-mm fines and the group A regolith

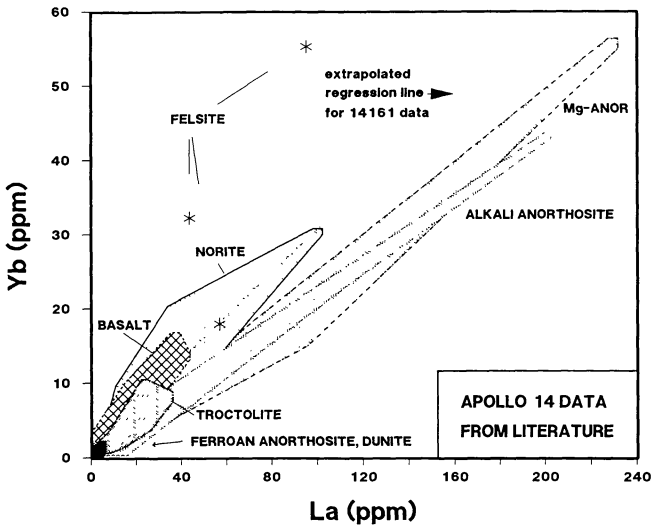

Fig. 12. Ranges of La and Yb concentrations in igneous monomict lithologies, from literature sources (see Fig. 7 for data references) and data on the 2-4-mm particles from 14161. The ranges for magnesian and alkali anorthosites are drawn out to high concentrations by only a few analyses, and lie along a trajectory toward the La and Yb concentrations of lunar whitlockite. The regression line is the same as in Fig. 10.

breccias might have been transported together to the Apollo 14 site as a thin "sheet." However, large samples of regolith breccias from Apollo 14 also have essentially the same compositions as the <1-mm fines (*Simonds et al.,* 1977; *Simon et al.,* 1989). Many of these are known to have been formed as long ago as 3.7 b.y. from ^{40}Ar-^{39}Ar studies (*Alexander and Kahl,* 1974), and may contain even older components as evidenced by the presence of excess fission Xe (*Drozd et al.,* 1976; *Bernatowicz et al.,* 1978). Substantial numbers of large regolith breccias were collected during the mission, so we must also consider whether many of the regolith breccia fragments, and even the bulk of the <1-mm fines, might be comminution products of larger chunks of ancient regolith breccias.

We suggest that most of the group A regolith breccia particles are not fragments of ancient breccias but were formed from the local soil after the formation of the ancient regolith breccias. Siderophile-element concentrations are slightly higher in the regolith breccia particles than in the <1-mm fines (Table 6), presumably consistent with further meteorite working of material of local origin. The standard deviations of elemental concentrations for this group of particles are extremely tight (Table 6); they differ only by a factor of ~2 from those for different aliquots of the <1-mm fines (14163) that are very well stirred. Such tight standard

TABLE 6. Mass-weighted mean composition of 2-4-mm soil fractions and <1-mm soil fines.

	14161 2-4 mm N=381	14163 <1-mm fines N=8		Light Impact Melt Breccia N=72		Regolith Breccia Group A N=69		14142/3 2-4 mm N=41	14141 <1 mm N=2
	Mean	Mean	Std. dev.	Mean	Std. dev.	Mean	Std. dev.	Mean	Mean
FeO	9.89	10.29	0.18	10.09	0.84	10.44	0.29	10.92	9.60
CaO	10.7	11.0	0.5	9.9	1.1	10.7	0.7	10.4	10.9
Na_2O	0.764	0.711	0.021	0.815	0.065	0.688	0.048	0.781	0.768
Sc	20.6	21.5	0.3	21.3	2.7	22.0	0.6	25.9	21.3
Cr	1246	1349	24	1253	139	1380	43	1444	1304
Co	32.7	35.2	2.0	34.4	10.9	36.0	5.1	32.0	27.2
Ni*	264-323	349	26	315-351	146	380-392	124	322	253
Zr	1166	1003	61	1303	363	1029	145	1097	1002
Cs	0.73	0.76	0.02	0.84	0.24	0.73	0.15	1.02	0.74
Ba	869	828	23	971	155	804	44	886	905
La	77.1	68.0	1.4	87.0	19.8	67.0	3.2	71.1	66.3
Sm	34.1	30.2	0.7	38.5	9.0	30.2	1.4	31.1	29.1
Eu	2.60	2.54	0.04	2.68	0.28	2.46	0.15	2.43	2.48
Tb	6.74	6.05	0.09	7.63	1.76	6.01	0.29	6.34	5.94
Yb	24.8	22.1	0.4	27.9	5.6	22.0	1.0	23.4	21.8
Lu	3.39	3.00	0.06	3.83	0.75	2.99	0.14	3.20	2.94
Hf	27.3	24.0	1.3	30.5	8.3	23.9	1.4	25.5	23.3
Ta	3.3	3.0	0.1	3.7	0.8	3.0	0.2	3.2	3.2
Ir†	7.3-10.8	11.6	1.8	5.4-9.0	5.6	10.2-11.9	7.8	7.9	6.4
Au†	4.3-6.9	5.7	0.5	5.4-7.2	4.9	5.1-5.8	3.1	4.9	7.6
Th	14.8	12.8	0.3	16.7	3.7	12.8	0.8	13.6	12.6
U	4.09	3.51	0.20	4.61	1.02	3.57	0.25	3.75	3.57
(Ir,Au)	(270,266)	(8,8)		(43,54)		(59,61)		(41,41)	(2,2)

* Nickel mean concentrations of the 2-4-mm particles in column 1 include less-than values and are therefore upper limits. Where a range is given, the upper limit is calculated as for column 1 and the lower limit is calculated assuming zero for a concentration rather than the less-than value.

† Gold and Ir mean concentrations are based on those samples for which concentrations were determined; (Ir,Au) is the number of determinations. Where a range is given, the lower limit is calculated assuming zero for those particles for which no concentration value was determined.

Oxides are in percent, Ir and Au in ppb, all others in ppm.

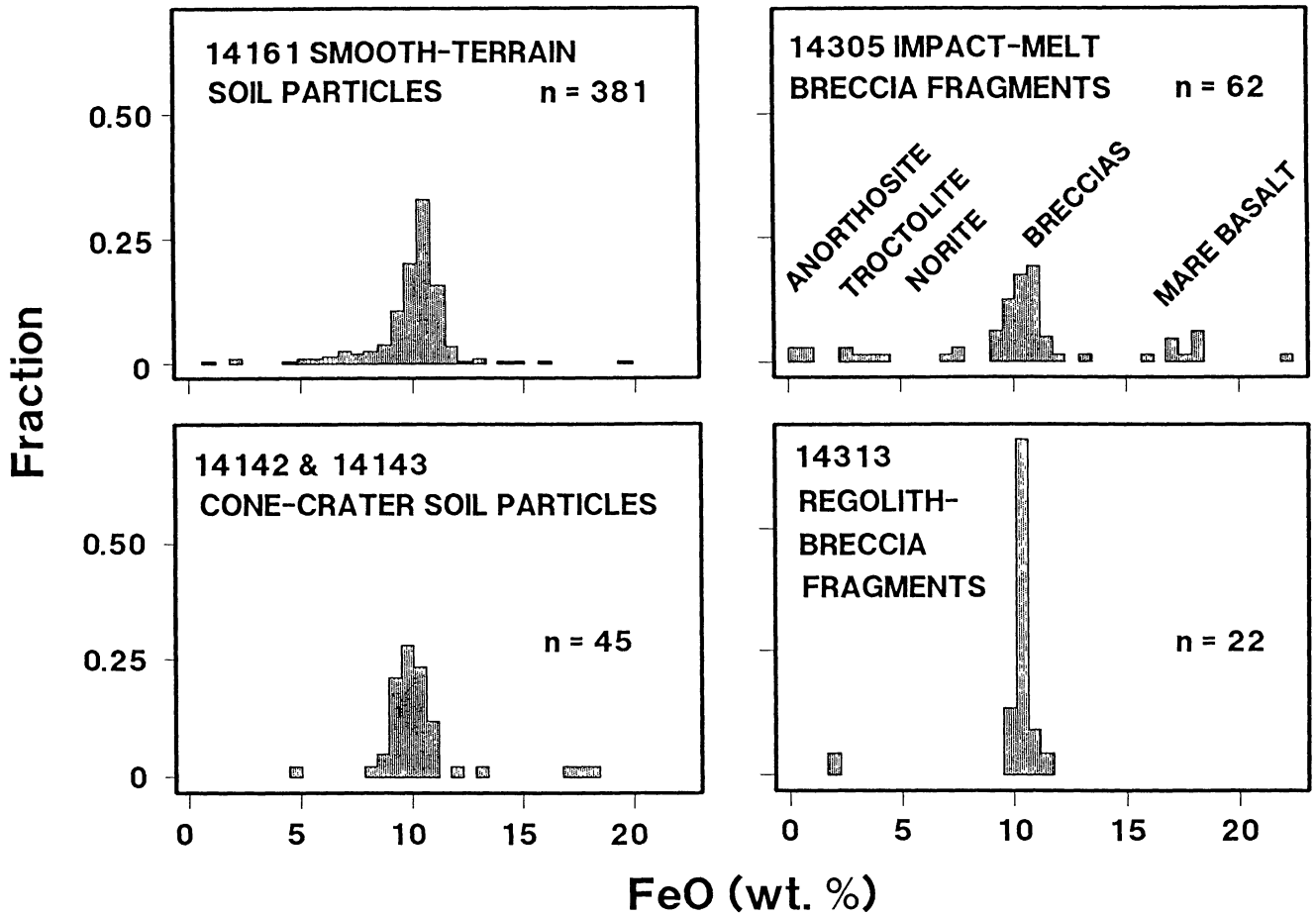

Fig. 13. Histogram of weight fraction of particles of given FeO concentration in 14161 2-4-mm, "smooth-terrain" particles; 14142/3 Cone Crater soil particles; 14305 impact-melt breccia fragments; and 14313 regolith breccia fragments. Iron-oxide concentrations are used as an approximation of the proportions of different lithologic components, as indicated for the 14305 plot. Sample 14305 is taken as an example of "Cone Crater breccias." In the plot of 14305 data, "breccias" equates to matrix compositions. The 14305 data include compositions from *Shervais et al.* (1984).

deviations are about what we would expect in sequential samples in the same soil layer in a core that presumably has not been stirred (e.g., *Korotev,* 1991). Values of I_s/FeO of the 2-4-mm regolith breccia particles are in the range of ~30-80 (R. V. Morris, personal communication, 1990), similar to the value for 14163 (I_s/FeO = 57) and other Apollo 14 soils from locations other than Cone Crater (*Morris et al.,* 1983). Finally, a high proportion of the surface area of some of these particles is glass, i.e., some of these particles are large agglutinates, soil fines bonded together by impact-produced glass. At least these agglutinitic particles may be regarded as particles that formed mainly in the 2-4-mm or slightly larger size range. We regard this as demonstrating that the regolith breccias of group A are local, *constructional* products in the >2-mm size range from finer material of the bulk soil.

The similarity in composition among the ancient regolith breccias, regolith breccia particles from 14161, and <1-mm fines from all Apollo 14 sites, including Cone Crater, indicates that all three materials have the same provenance. However, we do not know whether the bulk of the surface fines formed *in situ* or whether the fines were transported to the site along with the regolith breccias, but separately from materials that comprise deeper levels of the Fra Mauro Formation

Igneous Components of Polymict Materials

Samples returned from the Apollo 14 site are dominated by regolith and impact-melt breccias; endogenous igneous rocks are scarce and found almost exclusively as clasts in breccias and as small fragments in soil samples. Thus, it is difficult to ascertain directly what igneous rocks actually made up the pre-impact lunar crust from which the Apollo 14 samples were derived. As noted by previous workers (e.g., *Quaide and Wrigley,* 1972), the coarse grain size of monomineralic clasts in impact-derived breccias and the presence of nonbasaltic, crystalline, lithic fragments indicate plutonic source rocks. If we assume

that the breccia compositions were derived in a straightforward manner from mixing of igneous lithologies, then we can model these compositions as mixtures of compositions of known igneous rocks. It is probable that not all the appropriate igneous lithologies have been sampled or are represented among the returned lunar samples. Even lithic and mineral clasts within the breccias may not be representative of the bulk target lithologies. It is possible that breccia formation involves processes that mix rocks in such a way that original igneous compositions are either mechanically fractionated by nonmodal combinations of cataclastic lithologies, fractionated by impact-melt segregation and fractionation, or mixed nonmodally by differential partial melting and separation of melt from residue and injection of melt into other lithologies during impact. For the purpose of this paper, we begin with the assumption that polymict materials represent modal mixtures of source lithologies, although this does not imply that 2-4-mm particles are necessarily representative samples of the polymict breccias.

The distribution of ITE concentrations among the suite of polymict soil particles that have La concentrations greater than about 40 ppm La (Fig. 10, La vs. Yb) is one that we might expect from simple mixing between a major component with high ITE concentrations and a second major component with low ITE concentrations. However, the ITE do not correlate well with major elements or with compatible or "ferromagnesian" trace elements such as Sc and Cr (Fig. 11, Sc vs. La), nor do the major elements and compatible trace elements correlate as well with one another as do the ITE. Thus, mixtures of just two endmember compositions cannot explain the compositions of the polymict particles. The cause of the compositional scatter among the polymict particles might be that different 2-4-mm fragments have different proportions of individual components, all of whose ITE/ITE ratios are roughly similar, but whose ITE/compatible-element and ITE/major-element ratios are much more variable. In this approximation, the individual components are not premixed to yield a single average mixing component, but occur in variable proportions in different polymict particles. Variations in the proportion of a component with low ITE concentrations (e.g., mare basalt) would not have much effect on La/Yb, but would cause a substantial deviation from the average La/Sc.

First, we address whether the igneous lithologies represented by the monomict particles in the soil (14161) can account for the observed compositional scatter in compatible elements and major elements among the polymict particles. The compositional scatter could conceivably result from variations in the proportions of different minerals contained in the igneous lithologies. A higher ratio of pyroxene to plagioclase in a particular clast included in a 2-4-mm fragment could change the overall Sc concentration in the fragment by several ppm, which is about the range of scatter observed. Petrographic observations suggest that although coarse mineral clasts are present in some breccia particles, the clasts are generally too fine grained to accommodate this explanation.

The monomict lithologies found among the 2-4-mm particles, as a group, do not represent the low-ITE component because, as shown below, they do not contain high enough Sc concentrations *on average* to account for the *average* Sc concentrations of the polymict particles. The mean La and Sc concentrations of the suite of monomict particles in the soil plot in the larger shaded rectangle in Fig. 11 (also shown for La-Yb, Fig. 10). The shaded rectangle represents the standard error of the mean, based on the compositions of the monomict particles, excluding those with greater than ~90 ppm La and excluding the KREEP basalts. The mean of the KREEP basalts is shown separately by the smaller rectangle. The mean concentrations of Sc in the main groups of polymict particles are higher than expected if the ITE-rich component has La and Sc concentrations in about the same ratio as KREEP (*Warren,* 1989) and lie within the limits shown in Fig. 11. These limits were placed to include the shaded rectangles at low La concentrations and average high-K KREEP, QMD, and the ITE-rich melt rock.

The monomict particles with greater than ~20 ppm Sc are the VHK or aluminous mare basalts and basaltic glasses, QMD, and several norite and gabbronorite fragments, two of which have unusually high REE concentrations. Quartz monzodiorite would appear to be a potential source of Sc, but other compositional characteristics make it unsuitable as a major component of the polymict breccias (see next section). If mare basalt is a major source of Sc in the polymict breccias, it is an underrepresented component among the igneous fragments and must be finely dispersed and well mixed into the polymict particles, because there are no polymict particles in the 2-4-mm size range that are intermediate or mostly basaltic in composition. Mare basalt glasses are observed in Apollo 14 regolith breccias (*Delano,* 1988) and in soil fines (*McKay et al.,* 1972); thus we expect to find compositional evidence of a mare component in agglutinates and regolith breccia particles. None of the norite or gabbronorite compositions individually has a suitable composition to account for the Sc-rich average compositions of polymict particles, but taken as a group, these lithologies appear to have the best potential of being a principal component. We now extend these observations on Sc and La to multielement compositions through the use of mixing models.

Mixing Models

We approach the problem of the missing (or poorly constrained) igneous component(s) by detailed analysis of "mixed" compositions and modeling of the compositions as mixtures of known igneous lithologies, with special attention given to the model residuals. As a first approximation, we used the igneous rock types most closely associated with Apollo 14 soil and breccias as potential components. Using 14163 as a representative soil, we attempted to model the mean soil composition as a mixture of apparently monomict lithologies found among the 2-4-mm particles (14161).

An outcome of this exercise is the demonstration that some igneous lithologies cannot be volumetrically significant components of the polymict particles. We infer that these lithologies were not abundant at the site or region where these particles were assembled. To demonstrate this, we began with the least-squares method (*Bryan et al.,* 1969; *Boynton et al.,* 1975) to determine the best-fit proportions of subsets of components in a given polymict composition. When many components are present, this "inverse" method leads to results

of limited utility, because it cannot adequately distinguish compositionally similar components. Therefore, we next used a "forward" method of combining components in known or assumed proportions to determine the compositions of mixtures, beginning with the results of the least-squares mixing as guidelines. In this way, we can determine the "best fit" using a given set of components, as well as test the effects of variations in the proportions of one or several components. Different mixing solutions are compared by a residual sum of squares and a weighted residual sum of squares that accounts for relative analytical uncertainty, using the elements we analyze by INAA and estimates of the remaining major elements based on comparison to data from the literature and on modal recombination techniques based on microprobe analyses (e.g., *Vaniman et al.,* 1979). The "best fit" to a given mixing problem is not considered to be an acceptable solution if the residual sum of squares is high, but such solutions are useful because they indicate that a particular set of components may be inappropriate.

Limits on the proportions of some of the igneous components in the polymict materials are constrained by concentrations of certain key elements. For example, proportions of alkali anorthosite are constrained mainly by the concentrations of Na_2O and Eu, proportions of mare basalt are constrained by concentrations of Sc, and proportions of felsite are constrained by concentrations of Ba, Cs, Ta, Th, and U. Anorthositic lithologies in general are constrained by CaO and FeO concentrations, and ferroan anorthosite, in particular, by its low concentrations of most trace elements.

The high ITE concentrations of the polymict materials require an ITE-rich component. Among igneous fragments from 14161, the QMD fragment has a set of relative ITE concentrations similar to that of KREEP (*Warren and Wasson,* 1979), so it was initially tested as an ITE-rich component. We found it to be unsuitable as the only ITE-rich component on the basis of concentrations of major elements and Cr. We do not use the composition of "average high-K KREEP" as an ITE-rich component because it does not correspond directly to a specific igneous rock type.

Modeling the composition of the <1-mm soil. When mixed in proportions that give a "best fit," the igneous particles from 14161 do not yield a composition that sufficiently matches that of the <1-mm fines (based on 20 elements determined by INAA). The best-fit mixture contains concentrations of Na_2O, CaO, Cs, Zr, Hf, Th, and U that are too high, and concentrations of FeO, Cr, and Eu that are too low (Fig. 14a). To obtain a substantially improved solution, it is necessary to include a breccia composition as one of the mixing components. For this, we used an average impact-melt breccia composition instead of that of QMD as the component with high ITE concentrations (Fig. 14b). This implies the presence of an igneous component (or components) in the impact-melt breccias that is not observed as a discrete lithology among the igneous fragments in the 2-4-mm particles. Our results differ somewhat from those of others (e.g., *Laul et al.,* 1982; *Jerde et al.,* 1987; *Lingner et al.,* 1989) in that we use exclusively Apollo 14 materials as components and we use an average breccia composition rather than KREEP as the component with high ITE concentrations to model the soil composition. We also consider the concentrations of Eu, Ba, Th, and several other ITE that provide important constraints for several components as discussed above. While this model provides a greatly improved fit, it still does not provide a fully satisfactory fit, especially for Na_2O and FeO.

The important results of modeling the composition of the <1-mm soil are as follows: (1) Several key elements (CaO, FeO, and Eu) cannot be adequately balanced through the use of the 2-4-mm igneous components alone. (2) Inclusion of >5% ferroan anorthosite in the soil yields excessive CaO and too little FeO. (3) Inclusion of >2% alkali anorthosite yields excessive Na_2O and CaO. (4) Inclusion of >1% felsite yields too much Cs, Th, and U and too low a ratio of La/Yb. (5) There may be on the order of 8% troctolitic anorthosite component. (6) Mare basalt is the only well-characterized component other than QMD that has a Sc concentration substantially greater than that of the soil; the model requires 5-10% mare basalt, more than is found as discrete particles among the 2-4-mm fragments. Apparently the mare component is fine-grained and dispersed among the particles of regolith breccias and agglutinates, consistent with petrographic observations on <1-mm fines from several Apollo 14 soils (*McKay et al.,* 1972; *Quaide and Wrigley,* 1972; *Simon et al.,* 1982). Simon et al. also calculated that the mare component of the fines was greater than that which was observed petrographically.

Modeling the composition of impact-melt breccias. When impact-melt breccia was included as a component to improve the quality of the fit, it became the principal component (~60%) of the soil. An important corollary of our mixing model for the soil is that the average impact-melt breccia composition cannot be adequately modeled as a mixture of the igneous components found among the 2-4-mm particles. The best fit using these components to model the average impact-melt breccia composition yields a mixture that has unacceptably high concentrations of CaO and Na_2O, low concentrations of FeO, Cr, and Eu, and low La/Yb. Of course, a very good fit to the impact-melt breccia composition is obtained if average high-K KREEP (*Warren,* 1989) is used as the ITE-rich component, but the reason is that the composition of high-K KREEP was derived from Apollo 14 ITE-rich materials, which include breccias such as these, so the argument is circular. Assuming that the breccia composition can be modeled as a simple mixture of igneous rocks produced during endogenic magmatic differentiation (i.e., excluding chemical separations that might result from impact processes), then the breccia includes igneous precursors of the <1-mm fines that are not represented as discrete fragments among the 2-4-mm igneous particles.

In modeling Apollo 14 polymict materials, we are faced with a dilemma. The commonly used component with high ITE concentrations is "KREEP." However, the only endogenous KREEP-like materials are KREEP basalts, and these have ITE concentrations that are exceeded by most Apollo 14 breccias. The impact-melt rock 14161,7233 (Table 2) has ITE concentrations 2.5-3.5 times those of average high-K KREEP. This fragment also has very magnesian pyroxenes [Mg/(Mg + Fe): 0.65-0.73] in relation to the anorthite content of its plagioclase (An_{63-69}) (Fig. 6). When we use the bulk composition of this

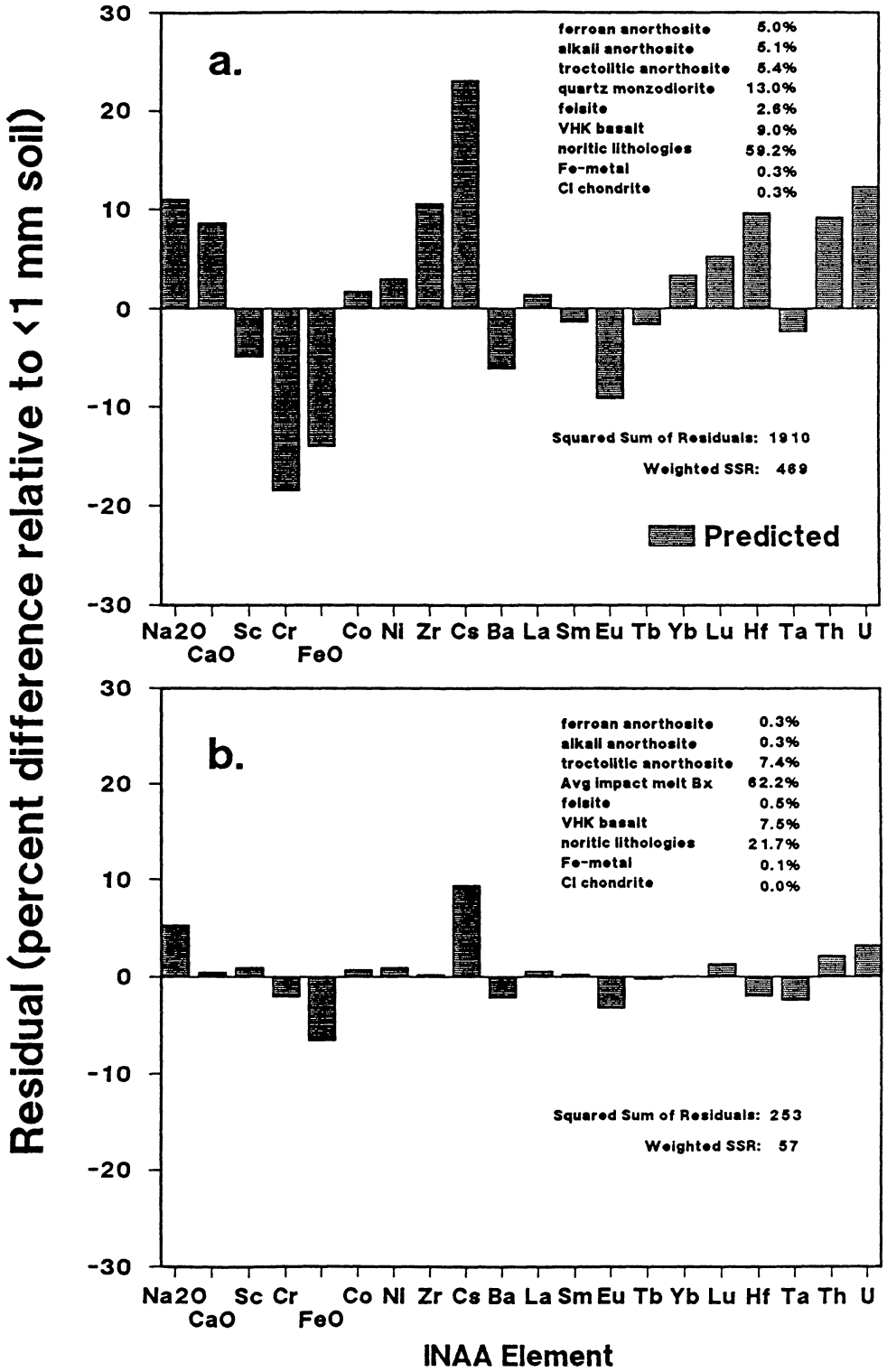

Fig. 14. Plot of predicted mixtures (percent difference) relative to composition being modeled, in this case, 14163 <1-mm fines. **(a)** Components include average compositions of igneous lithologies from 14161 2-4-mm particles. **(b)** Average light impact-melt breccia composition (Table 6) is used as the component with high ITE-concentrations. By using a more typical aluminous basalt such as 14072 as the mare basalt component, a slightly improved fit is obtained, particularly for Cs and somewhat for Fe, but the main features of the residual composition remain. This modification also requires an increase in the proportion of alkali anorthosite to ~2% and CI chondrite to ~0.2%. Composition of CI chondrite from *Wasson* (1985); composition of Fe metal from *Wlotzka et al.* (1972).

particle as the component with high ITE concentrations, the principal effect is to require only about one-third the amount of the ITE-rich component, i.e., ~16% rather than 50%, that has commonly been suggested in past studies of Apollo 14 materials (e.g., *Lindstrom et al.,* 1972; *Lingner et al.,* 1989). As a result, the major-element composition of this component is not such a dominant factor in the mixture.

Modeling of the average composition of impact-melt breccias yields constraints on the allowable proportions of known igneous lithologies in the source region of these breccias, and the model residuals indicate the compositional nature of the cryptic component. We use an average composition based on analyses of ~70 2-4-mm IMBx particles (Table 6). As components, we consider ferroan anorthosite, "Mg-suite" anorthosite, alkali anorthosite, troctolitic anorthosite, norite, felsite, aluminous mare basalt, KREEP basalt, felsite, QMD, Fe-metal, C1 chondrite, and as the high-ITE component, the ITE-rich impact-melt rock, 14161,7233. With this many components and some 20 elements, there are no unique, "best-fit" solutions. However, many different combinations of components yield the following general constraints, based mainly on the elements in parentheses: alkali anorthosite <10% (Na, Eu); felsite <5% (Ba, Cs, Ta, Th, U, etc.); aluminous mare basalt <8% (Sc, Cr). The presence of anorthosite of any variety is difficult to reconcile with that of other necessarily abundant components due to CaO and FeO mass balances. The only potential component that can balance high CaO and low FeO is mare basalt, which is constrained to 8%, as mentioned above. A greater proportion of troctolitic or noritic anorthosite than of anorthosite sensu stricto can be tolerated (e.g., 10%). Iron-metal and chondrite compositions fit the siderophile elements very well. Those components with compositions most similar to the IMBx composition are the most difficult to constrain. If we use the compositions of impact-melt rock 14161,7233 as the ITE-rich component, then norite or gabbroic norite (or a compositionally similar lithology) must be the major component, e.g., >50%, but of the monomict materials at Apollo 14, none has a composition that satisfactorily combines with the other components.

In addition to samples from 14161, we have considered as components compositions of rocks and clasts of other Apollo 14 samples taken from the literature. In either case, we cannot satisfactorily match the average IMBx composition. No matter what combination of components we select, the best fits yield mixtures with low-transition metal concentrations (Sc, Cr, Fe) and low Eu concentrations.

Based on our modeling, we predict that the cryptic component is mafic and has relatively high Sc, Cr, and Fe concentrations and is less magnesian than the noritic igneous rocks that have been found among the samples. In our modeling, we cannot balance Eu with alkali anorthosite without exacerbating the CaO and FeO mismatch. Thus, we also predict that the ferroan mafic component is relatively rich in Eu.

CONCLUSIONS

1. We have determined the lithologic and compositional distribution of 381 2-4-mm particles from 14161. The most abundant particles are the impact-melt lithologies (~50% by weight), mainly impact-melt breccias, but including impact-melt rocks and glasses. Regolith breccias and fragmental breccias make up another 40% of the particles. About 8% of the 2-4-mm particles are "mostly monomict" igneous lithologies.

2. Among the particles that appear to be monomict and igneous, fragments of mare basalt, troctolite, and alkali suite lithologies are rare, indicating that the surface layer of the Fra Mauro Formation was derived from a different portion of the lunar crust than the level excavated by the formation of Cone Crater (cf. *Stöffler et al.,* 1989).

3. The mean composition of the entire suite of 2-4-mm particles differs from that of the associated <1-mm fines by having higher concentrations of incompatible trace elements and Na_2O, and a lower concentration of CaO. This probably results from a higher proportion of ITE-rich impact-melt breccias in the 2-4-mm particles than in the <1-mm fines.

4. There is a subset of regolith breccia particles and agglutinates in the 2-4-mm particles that have nearly identical compositions and similar I_s/FeO to those of the <1-mm fines, but have siderophile-element concentrations slightly higher than the fines. These features suggest that these particles are constructional products formed from the local regolith rather than comminuted fragments of ancient regolith breccias.

5. Incompatible-trace-element compositions of the entire suite of 2-4-mm particles are consistent with mixing of a group of igneous components that have relatively low ITE concentrations with a component that has high ITE concentrations and fixed concentration ratios for the ITE. Compatible- and major-element compositions are more complex and probably result from variations in the relative proportions of "ITE-poor" components. However, the group of igneous components, in the proportions found in the 2-4-mm particles, cannot account for the average compositions of the main groups of polymict particles.

6. The composition of the associated <1-mm fines cannot be adequately modeled as a mixture of the igneous lithologies identified among the 2-4-mm particles. By including the average impact-melt breccia composition as a model component (the ITE-rich component), the composition of the <1-mm fines can be closely matched; however, the impact-melt breccias then become the principal component (~60%) of the soil. The results of these models suggest that the Apollo 14 subregolith basement or "bedrock" and the impact-melt breccias contain a compositionally distinct (high FeO, Cr, Sc, and Eu concentrations) but unidentified or unrecognized igneous component.

The distribution of compositions of the Fra Mauro materials and the distribution of lithologies as found in the suite of 2-4-mm particles from 14161 pose a fundamental question. If we interpret the source lithologies of Fra Mauro materials in the context of products formed by solidification of a magma ocean, and if the impact-generated polymict materials are a mixture of crustal lithologies with materials rich in KREEP from a deep crustal layer that was exhumed by a basin-forming impact, then crustal lithologies, especially ferroan anorthosite, should figure more prominently as components. The apparent paucity of ferroan anorthosite and of anorthosite in general among the igneous components that appear to have made up

the impact-melt breccias requires a substantial crustal section made up of other lithologies, chiefly noritic and gabbroic lithologies of the plutonic Mg-suite (cf. *Shervais et al.,* 1983).

We are doing detailed petrographic and compositional analyses of particles within different lithologic groups to improve our understanding of which lithologic components are actually represented as clasts in the breccias, and to identify the compositional characteristics of "cryptic" components that may no longer be directly represented in the polymict materials.

Acknowledgments. This research was funded through NASA grant NAG-956. We thank the Lunar Curatorial Facility at NASA Johnson Space Center for the preparation of 47 polished thin sections. Helpful comments from S. Simon, M. Lindstrom, and P. Warren have improved the manuscript. The comments and expeditious handling of the manuscript by associate editor D. Lindstrom are also appreciated.

REFERENCES

Alexander E. C. Jr. and Kahl S. B. (1974) ^{40}Ar-^{39}Ar studies of lunar breccias. *Proc. Lunar Sci. Conf. 5th,* pp. 1353-1373.

Bernatowicz T. J., Hohenberg C. M., Hudson B., Kennedy B. M., and Podosek F. A. (1978) Excess fission xenon at Apollo 16. *Proc. Lunar Planet. Sci. Conf. 9th,* pp. 1571-1597.

Boynton W. V., Baedecker P. A., Chou C.-L., Robinson K. L., and Wasson J. T. (1975) Mixing and transport of lunar surface materials: Evidence obtained by the determination of lithophile, siderophile, and volatile elements. *Proc. Lunar Sci. Conf. 6th,* pp. 2241-2259.

Brunfelt A. O., Heier K. S., Nilssen B., Sundvoll B., and Steinnes E. (1972) Distribution of elements between phases of Apollo 14 rocks and soils. *Proc. Lunar Sci. Conf. 3rd,* pp. 1133-1148.

Bryan W. B., Finger L. W., and Chayes F. (1969) Estimating proportions in petrographic mixing equations by least-squares approximation. *Science, 163,* 926-927.

Delano J. W. (1988) Apollo 14 regolith breccias: Different glass populations and their potential for charting space/time variations. *Proc. Lunar Planet. Sci. Conf. 18th,* pp. 59-65.

Dickinson T., Taylor G. J., Keil K., Schmitt R. A., Hughes S. S., and Smith M. R. (1984) Apollo 14 aluminous mare basalts and their possible relationship to KREEP. *Proc. Lunar Planet Sci. Conf. 15th,* in *J. Geophys. Res., 90,* C365-C374.

Drozd R. J., Kennedy B. M., Morgan C. J., Podosek F. A., and Taylor G. J. (1976) The excess fission xenon problem in lunar samples. *Proc. Lunar Sci. Conf. 7th,* pp. 599-623.

Engelhardt W. von, Arndt J., Stöffler D., and Schneider H. (1972) Apollo 14 regolith and fragmental rocks, their compositions and origin by impacts. *Proc. Lunar Sci. Conf. 3rd,* pp. 753-770.

Goodrich C. A., Taylor G. J., Keil K., Kallemeyn G. W., and Warren P. W. (1986) Alkali norite, troctolites, and VHK mare basalts from breccia 14304. *Proc. Lunar Planet Sci. Conf. 16th,* in *J. Geophys Res., 91,* D305-D315.

Haskin L. A., Helmke P. A., Blanchard D. P., Jacobs J. W., and Telander K. (1973) Major and trace element abundances in samples from the lunar highlands. *Proc. Lunar Sci. Conf. 4th,* pp. 1275-1296.

Helmke P. A., Haskin L. A., Korotev R. L., and Ziege K. (1972) Rare earths and other trace elements in Apollo 14 samples. *Proc. Lunar Sci. Conf. 3rd,* pp. 1275-1292.

Hertogen J., Janssens M.-J., Takahashi H., Palme H., and Anders A. (1977) Lunar basins and craters: Evidence for systematic compositional changes of the bombarding population. *Proc. Lunar Sci. Conf. 8th,* pp. 17-45.

Hubbard N. J., Gast P. W., Rhodes J. M., Bansal B. M., and Wiesmann H. (1972) Nonmare basalts: Part II. *Proc. Lunar Sci. Conf. 3rd,* pp. 1161-1179.

James O. B. and Hammarstrom J. G. (1977) Petrology of four clasts from Consortium Breccia 73215. *Proc. Lunar Sci. Conf. 8th,* pp. 2459-2494.

Jerde E. A., Warren P. H., Morris R. V., Heiken G. H., and Vaniman D. T. (1987) A potpourri or regolith breccias: "New" samples from the Apollo 14, 16, and 17 landing sites. *Proc. Lunar Planet Sci. Conf. 17th,* in *J. Geophys. Res., 92,* E526-E536.

Jolliff B. L. (1990) Fragments of quartz monzodiorite and felsite in Apollo 14 soil particles (abstract). In *Lunar and Planetary Science XXI,* pp. 571-572. Lunar and Planetary Institute, Houston.

Jolliff B. L. (1991) Fragments of quartz monzodiorite and felsite in Apollo 14 soil particles. *Proc. Lunar Planet. Sci., Volume 21,* this volume.

Korotev R. L. (1991) Geochemical stratigraphy of two regolith cores from the central highlands of the Moon. *Proc. Lunar Planet. Sci., Volume 21,* this volume.

Laul J. C., Wakita H., Showalter D. L., Boynton W. V., and Schmitt R. A. (1972) Bulk, rare earth, and other trace elements in Apollo 14 clastic materials. *Proc. Lunar Sci. Conf. 3rd,* pp. 1181-1200.

Laul J. C., Papike J. J., and Simon S. B. (1982) The Apollo 14 regolith: Chemistry of cores 14210/14211 and 14220 and soils 14141, 14148 and 14149. Proc. *Lunar Planet. Sci. Conf. 13th,* in *J. Geophys. Res., 87,* A247-A259.

Laul J. C., Gosselin D. C., Galbreath K. C., Simon S. B., and Papike J. J. (1989) Chemistry and petrology of Apollo 17 highland coarse fines: plutonic and melt rocks. *Proc. Lunar Planet. Sci. Conf. 19th,* pp. 85-97.

Lindstrom D. J. and Korotev R. L. (1982) TEABAGS: Computer programs for instrumental neutron activation analysis. *J. Radioanal. Nucl. Chem., 70,* 439-458.

Lindstrom M. M., Duncan A. R., Fruchter J. S., McKay S. M., Stoeser J. W., Goles G. G., and Lindstrom D. J. (1972) Compositional characteristics of some Apollo 14 clastic materials. *Proc. Lunar Sci. Conf. 3rd,* pp. 1201-1214.

Lindstrom M. M., Knapp S. A., Shervais J. W., and Taylor L. A. (1984) Magnesian anorthosites and associated troctolites and dunite in Apollo 14 breccias. *Proc. Lunar Planet Sci. Conf. 15th,* in *J. Geophys. Res., 89,* C41-C49.

Lindstrom M. M., Marvin U. B., Vetter S. K., and Shervais J. W. (1988) Apennine Front revisited: Diversity of Apollo 15 highland rock types. *Proc. Lunar Planet. Sci. Conf. 18th,* pp. 169-185.

Lingner S., Spettel B., and Stöffler D. (1989) Fra Mauro Formation, Apollo 14: III. Calculated composition of the primordial lunar crust in the Imbrium region (abstract). In *Workshop on Moon in Transition: Apollo 14, KREEP, and Evolved Lunar Rocks* (G. J. Taylor and P. H. Warren, eds.), pp. 62-65. LPI Tech. Rpt. 89-03, Lunar and Planetary Institute, Houston.

McKay D. S., Heiken G. H., Taylor R. M., Clanton U. S., Morrison D. A., and Ladle G. H. (1972) Apollo 14 soils: Size distribution and particle types. *Proc. Lunar Sci. Conf. 3rd,* pp. 983-994.

McKay G. A., Wiesmann H., Nyquist L. E., Wooden J. L., and Bansal B. M. (1978) Petrology, chemistry, and chronology of 14078: chemical constraints on the origin of KREEP. *Proc. Lunar Planet. Sci. Conf. 9th,* pp. 661-687.

McKay G. A., Wiesmann H., Bansal B. M., and Shih C.-Y. (1979) Petrology, chemistry, and chronology of Apollo 14 KREEP basalts. *Proc. Lunar Planet. Sci. Conf. 10th,* pp. 181-205.

Morris R. V. (1976) Surface exposure indices of lunar soils: A comparative FMR study. *Proc. Lunar Sci. Conf. 7th,* pp. 315-335.

Morris R. V., Score R., Dardano C., and Heiken G. (1983) *Handbook of Lunar Soils.* Planetary Materials Branch Publ. No. 67, NASA Johnson Space Center, Houston. 914 pp.

Neal C. R., Taylor L. A., and Lindstrom M. M. (1988) Apollo 14 mare basalt petrogenesis: Assimilation of KREEP-like components by a

fractionating magma. *Proc. Lunar Planet Sci. Conf. 18th,* pp. 139-153.

Papike J. J., Simon S. B., White C., and Laul J. C. (1981) The relationship of the lunar regolith <10 μm fraction and agglutinates. Part I: A model for agglutinate formation and some indirect supportive evidence. *Proc. Lunar Planet. Sci. 12B,* pp. 409-420.

Pieters C. M. (1989) Craters as probes to the interior: Unexpected complexity of the Lunar Crust from near-infrared spectroscopy (abstract). *EOS Trans. AGU, 70,* 378.

Powell B. N. and Weiblen P. W. (1972) Petrology and origin of lithic fragments in the Apollo 14 regolith. *Proc. Lunar Sci. Conf. 3rd,* pp. 837-852.

Quaide W. and Wrigley R. (1972) Mineralogy and origin of Fra Mauro fines and breccias. *Proc. Lunar Sci. Conf. 3rd,* pp. 771-784.

Rose H. J. Jr., Cuttitta F., Annell C. S., Carron M. K., Christian R. P., Dwornik E. J., Greenland L. P., and Ligon D. T. Jr. (1972) Compositional data for twenty-one Fra Mauro lunar materials. *Proc. Lunar Sci. Conf. 3rd,* pp. 1215-1230.

Ryder G. (1976) Lunar sample 15405: Remnant of a KREEP basalt-granite differentiated pluton. *Earth Planet. Sci. Lett., 29,* 255-268.

Ryder G. (1987) Petrographic evidence for nonlinear cooling rates and a volcanic origin for Apollo 15 KREEP basalts. *Proc. Lunar Planet Sci. Conf. 17th,* in *J. Geophys. Res. 92,* E331-E339.

Ryder G. and Spudis P. D. (1987) Chemical composition and origin of Apollo 15 impact melts. *Proc. Lunar Planet Sci. Conf. 17th,* in *J. Geophys. Res., 92,* E432-E446.

Ryder G., Norman M. D., and Score R. (1980) The distinction of pristine from meteorite-contaminated highlands rocks using metal compositions. *Proc. Lunar Planet. Sci. Conf. 11th,* pp. 471-479.

Shervais J. W. (1989) Highland crust at the Apollo 14 site: A review (abstract). In *Workshop on Moon in Transition: Apollo 14, KREEP, and Evolved Lunar Rocks* (G. J. Taylor and P. H. Warren, eds.), pp. 118-127. LPI Tech. Rpt. 89-03, Lunar and Planetary Institute, Houston.

Shervais J. W., Taylor L. A., and Laul J. C. (1983) Ancient crustal components in the Fra Mauro breccias. *Proc. Lunar Planet Sci. Conf. 14th,* in *J. Geophys. Res., 88,* B177-B192.

Shervais J. W., Taylor L. A., Laul J. C., and Smith M. R. (1984) Pristine highland clasts in Consortium Breccia 14305: Petrology and geochemistry. *Proc. Lunar Planet. Sci. Conf. 15th,* in *J. Geophys. Res., 89,* C25-C40.

Shervais J. W., Taylor L. A., and Lindstrom M. M. (1985a) Apollo 14 mare basalts: Petrology and geochemistry of clasts from Consortium breccia 14321. *Proc. Lunar Planet. Sci. Conf. 15th,* in *J. Geophys Res., 90,* C375-C395.

Shervais J. W., Taylor L. A., Laul J. C., Shih C.-Y., and Nyquist L. E. (1985b) Very high potassium (VHK) basalt: Complications in mare basalt petrogenesis. *Proc. Lunar Planet. Sci. Conf. 16th,* in *J. Geophys. Res., 90,* D3-D18.

Simon S. B., Papike J. J., and Laul J. C. (1981) The lunar regolith: Comparative studies of the Apollo and Luna sites. Petrology of soils from Apollo 17, Luna 16, 20, and 24. *Proc. Lunar Planet. Sci. 12B,* pp. 371-388.

Simon S. B., Papike J. J., and Laul J. C. (1982) The Apollo 14 regolith: Petrology of cores 14210/14211 and 14220 and soils 14141, 14148, and 14149. *Proc. Lunar Planet. Sci. Conf. 13th,* in *J. Geophys. Res., 87,* A232-A246.

Simon S. B., Papike J. J., Shearer C. K., Hughes S. S., and Schmitt R. A. (1989) Petrology of Apollo 14 regolith breccias and ion microprobe studies of glass beads. *Proc. Lunar Planet. Sci. Conf. 19th,* pp. 1-17.

Simonds C. H., Phinney W. C., Warren J. L., McGee P. E., Geeslin J., Brown R. W., and Rhodes J. M. (1977) Apollo 14 revisited, or breccias aren't so bad after all. *Proc Lunar Sci. Conf. 8th,* pp. 1869-1893.

Stöffler D., Knöll H.-D., Marvin U. B., Simonds C. H., and Warren P. W. (1980) Recommended classification and nomenclature of lunar highland rocks—a committee report. In *Proceedings of the Conference on the Lunar Highlands Crust* (J. J. Papike and R. B. Merrill, eds.), pp. 51-70. Pergamon, New York.

Stöffler D., Lingner S., Heusser K., Jessberger E. K., Palme H., Spettel B., and Wänke H. (1986) Cone Crater Consortium, Apollo 14: (2) Precursor igneous rocks and ages of polymict breccias (abstract). In *Lunar and Planetary Science XVII,* pp. 829-830. Lunar and Planetary Institute, Houston.

Stöffler D., Bobe K. D., Jessberger E. K., Lingner S., Palme H., Spettel B., Stadermann F., and Wänke H. (1989) Fra Mauro Formation, Apollo 14: IV. Synopsis and synthesis of consortium studies (abstract). In *Workshop on Moon in Transition: Apollo 14, KREEP, and Evolved Lunar Rocks* (G. J. Taylor and P. H. Warren, eds), pp. 145-148. LPI Tech. Rpt. 89-03, Lunar and Planetary Institute, Houston.

Taylor G. J., Warner R. D., Keil K., Ma M.-S., and Schmitt R. A. (1980) Silicate liquid immiscibility, evolved lunar rocks and the formation of KREEP. In *Proceedings of the Conference on the Lunar Highlands Crust* (J. J. Papike and R. B. Merrill, eds.), pp. 339-352. Pergamon, New York.

Taylor S. R., Kaye M., Muir P., Nance W., Rudowski R., and Ware N. (1972) Composition of the lunar uplands: chemistry of Apollo 14 samples from Fra Mauro. *Proc. Lunar Sci. Conf. 3rd,* pp. 1231-1250.

Vaniman D. T. and Papike J. J. (1980) Lunar highland melt rocks: Chemistry, petrology and silicate mineralogy. In *Proceedings of the Conference on the Lunar Highlands Crust* (J. J. Papike and R. B. Merrill, eds.), pp. 271-337. Pergamon, New York.

Vaniman D. T., Papike J. J., and Schweitzer E. L. (1978) The Apollo 16 drive tube 60009/60010. Part II: Petrology and major element partitioning among the regolith components. *Proc. Lunar Planet. Sci. Conf. 9th,* pp. 1827-1860.

Wänke H., Baddenhausen H., Balacescu A., Teschke F., Spettel B., Dreibus G., Palme H., Quijano-Rico M., Kruse H., Wlotzka F., and Begemann F. (1972) Multielement analyses of lunar samples and some implications of the results. *Proc. Lunar Sci. Conf. 3rd,* pp. 1251-1268.

Warner J. L. (1972) Metamorphism of Apollo 14 breccias. *Proc. Lunar Sci. Conf. 3rd,* pp. 623-643.

Warner R. D., Taylor G. J., Keil K., Ma M.-S., and Schmitt R. A. (1980) Aluminous mare basalts: New data from Apollo 14 coarse fines. *Proc. Lunar Planet. Sci. Conf. 11th,* pp. 87-104.

Warren P. H. (1989) KREEP: Major-element diversity, trace-element uniformity (almost) (abstract). In *Workshop on Moon in Transition: Apollo 14, KREEP, and Evolved Lunar Rocks* (G. J. Taylor and P. H. Warren, eds.), pp. 149-153. LPI Tech. Rpt. 89-03, Lunar and Planetary Institute, Houston.

Warren P. H. and Wasson J. T. (1977) Pristine nonmare rocks and the nature of the lunar crust. *Proc. Lunar Sci. Conf. 8th,* pp. 2215-2235.

Warren P. H. and Wasson J. T. (1979) The origin of KREEP. *Rev. Geophys. Space Phys., 17,* 73-88.

Warren P. H. and Wasson J. T. (1980) Further foraging for pristine nonmare rocks: Correlations between geochemistry and longitude. *Proc. Lunar Planet. Sci. Conf. 11th,* pp. 431-470.

Warren P. H., Taylor G. J., Keil K., Kallemeyn G. W., Rosener P. S., and Wasson J. T. (1983a) Sixth foray for pristine nonmare rocks and an assessment of the diversity of lunar anorthosites. *Proc. Lunar Planet. Sci. Conf. 13th,* in *J. Geophys. Res., 88,* A615-A630.

Warren P. H., Taylor G. J., Keil K., Marshall C., and Wasson J. T. (1981) Foraging westward for pristine nonmare rocks: Complications for petrogenetic models. *Proc. Lunar Planet. Sci. 12B,* pp. 21-40.

Warren P. H., Taylor G. J., Keil K., Kallemeyn G. W., Shirley D. N., and Wasson J. T. (1983b) Seventh foray: whitlockite-rich lithologies, a diopside-bearing troctolitic anorthosite, ferroan anorthosites, and

KREEP. *Proc. Lunar Planet. Sci. Conf. 14th,* in *J. Geophys. Res., 88,* B151-B164.

Warren P. H., Taylor G. J., Keil K., Shirley D. N., and Wasson J. T. (1983c) Petrology and chemistry of two "large" granite clasts from the Moon. *Earth Planet. Sci. Lett., 64,* 175-185.

Warren P. H., Shirley D. N., and Kallemeyn G. W. (1986) A potpourri of pristine moon rocks, including a VHK mare basalt and a unique, augite-rich Apollo 17 anorthosite. *Proc. Lunar Planet. Sci. Conf. 16th,* in *J. Geophys. Res., 91,* D319-D330.

Warren P. H., Jerde E. A., and Kallemeyn G. W. (1987) Pristine moon rocks: a "large" felsite and a metal-rich ferroan anorthosite. *Proc. Lunar Planet. Sci. Conf. 17th,* in *J. Geophys. Res., 92,* E303-E313.

Wasson J. T. (1985) *Meteorites: Their Record of Early Solar-System History.* Freeman, New York. 267 pp.

Wilshire H. G. and Jackson E. D. (1972) Petrology of the Fra Mauro formation at the Apollo 14 landing site (abstract). In *Lunar Science III,* pp. 803-805. The Lunar Science Institute, Houston.

Wlotzka F., Jagoutz E., Spettel B., Baddenhausen H., Balacescu A., and Wänke H. (1972) On lunar metallic particles and their contribution to the trace element content of Apollo 14 and 15 soils. *Proc. Lunar Sci. Conf. 3rd,* pp. 1077-1084.

Wlotzka F., Spettel B., and Wänke H. (1973) On the composition of metal from Apollo 16 fines and the meteoritic component. *Proc. Lunar Sci. Conf. 4th,* pp. 1483-1491.